Journal of Molecular Structure 1165 (2018) 162–176

Contents lists available at ScienceDirect

Journal of Molecular Structure

journal homepage: http://www.elsevier.com/locate/molstruc

# Design, synthesis, antioxidant properties and mechanism of action of new N,N′-disubstituted benzimidazole-2-thione hydrazone derivatives

Neda O. Anastassova [a, *], Denista Y. Yancheva [a], Anelia Ts Mavrova [b], Magdalena S. Kondeva-Burdina [c], Virginia I. Tzankova [c], Nadya G. Hristova-Avakumova [d], Vera A. Hadjimitova [d]

[a] Institute of Organic Chemistry with Centre of Phytochemistry, Bulgarian Academy of Sciences, Acad. G. Bonchev Str., build. 9, 1113 Sofia, Bulgaria
[b] University of Chemical Technology and Metallurgy, 8 Kliment Ohridski Blvd., 1756 Sofia, Bulgaria
[c] Laboratory "Drug Metabolism and Drug Toxicity", Department of Pharmacology, Pharmacotherapy and Toxicology, Faculty of Pharmacy, Medical University of Sofia, 2 Dunav Str., 1000 Sofia, Bulgaria
[d] Department of Medical Physics and Biophysics, Faculty of Medicine, Medical University of Sofia, 2 Zdrave Str., 1431 Sofia, Bulgaria

ARTICLE INFO

*Article history:*
Received 8 February 2018
Received in revised form
26 March 2018
Accepted 27 March 2018
Available online 28 March 2018

*Keywords:*
1,3-Disubstituted benzimidazole-2-thiones
Hydrazones
Antioxidant
Hepatoprotection
Oxidative stress

ABSTRACT

New series of N,N′-disubstituted benzimidazole-2-thione were synthesized by introduction of hydrazone moiety in the side chains. The toxicological potential of studied compounds was evaluated by monitoring the cell viability and levels of lactate dehydrogenase, glutathione and malonaldehyde in isolated rat hepatocytes. The antioxidant properties of the compounds with the lowest toxicity were evaluated using oxidative stress induced by *tert*-butylhydroperoxide (*tert*-BOOH) on rat hepatocytes. The unsubstituted benzimidazole-2-thiones containing methoxyphenyl moieties, which revealed the lowest cytotoxic effects on isolated rat hepatocytes, exhibited statistically significant cytoprotective and antioxidant effects similar to those of quercetin. The elucidation of the antioxidant activity of the tested hydrazones was complimented by evaluation of their protective effect against iron induced oxidative damage in classic model systems containing basic biologically relevant molecules – lecithin and deoxyribose. It was demonstrated that all the tested compounds have protective effect on Fe (II) oxidative stress cellular damage of cellular lipids. DFT calculations were applied in order to calculate the reaction enthalpies of hydrogen atom abstraction and single-electron transfer in nonpolar and polar medium and to estimate the most probable mechanisms of free-radicals scavenging in comparison with those suggested for melatonin. The membrane permeability of the studied compounds was characterized based on calculated physico-chemical properties such as polar surface area, molecular weight, number of rotatable bonds and number of hydrogen-bond acceptors and donors.



## 1. Introduction

Redox imbalance in liver is the cause for alcoholic and nonalcoholic fatty liver disease, hepatic encephalopathy, liver fibroproliferative diseases and hepatitis C [1]. The application of antioxidant therapeutic agents is a rational curative strategy to prevent and cure such conditions [1–3]. Melatonin (N-acetyl-5-methoxytriptamine), a pineal gland hormone, can be used as additional therapy for influence the liver pathophysiological conditions due to its strong direct and indirect antioxidant properties [4–6]. Melatonin exerts a broad range of physiological and protective antioxidant effects, preventing the peroxidation of membrane lipids and protecting the proteins and DNA from oxidative damage induced by free radicals [7–9]. Beside direct free-radical scavenging properties, it also shows indirect antioxidative effects through the upregulation of several antioxidative enzymes. Melatonin has been found to be more effective than vitamin E in limiting lipid membrane destruction [9,10], serving as a natural mitochondria-targeted protective molecule [11]. It has been further proven that melatonin acts as a cytoprotector by inhibiting the

* Corresponding author.
*E-mail address:* neda.anastassova@gmail.com (N.O. Anastassova).

https://doi.org/10.1016/j.molstruc.2018.03.119
0022-2860/

apoptotic and oxidative processes and activating survival pathways in mouse hepatocytes that have undergone Fas-ligand apoptosis [6].

Having in mind all these beneficial features, in our previous study series of esters and hydrazides of the N,N′-disubstituted benzimidazole-2-thione were synthesized as melatonin analogues using a new method based on *aza*-Michael addition [12]. The hepatoprotective and antioxidant properties of the compounds were evaluated in a model of *tert*-butyl hydroperoxide-induced oxidative stress by measuring the parameters characterizing the functional-metabolic status of isolated rat hepatocytes including the cell viability, LDH leakage, GSH depletion and MDA production. Two of the studied compounds containing benzoyl moiety at position 5 of the benzimidazole ring exhibited the lowest cytotoxic and highest hepatoprotective and antioxidant effects similar to those of quercetin. Carried DFT calculations have revealed the most probable mechanism of antioxidant action. The results have encouraged us to continue investigating the N,N′-disubstituted benzimidazole-2-thione derivatives as potential hepatoprotective and antioxidant drugs with application for the treatment of liver disorders by synthesising series of hydrazones.

The strategy to design new antioxidants based on the structural similarity between N-substituted benzimidazole derivatives and melatonin demonstrated promising results in previous studies [13–15] Hydrazide and hydrazone melatonin analogues containing an o- and m-halogenated aromatic side chain were tested against hydrogen peroxide-induced lipid peroxidation and demonstrated significant antioxidant activity, even higher than melatonin itself [14]. The introduction of hydrazone side chains also increased the antioxidant activity of indoles compared to those of melatonin which could be due to the increased delocalization of the electrons which on its part promotes the scavenging of free radicals [15]. In another study halogene containing hydrazine derivatives of melatonin exhibited up to 95% strong inhibitory effect on the superoxide radical scavenging assay [16,17].

Therefore we have synthesized new N,N′-disubstituted benzimidazole-2-thiones by the introduction of hydrazone moiety in the side chains and have studied their hepatoprotective activity in *tert*-butyl hydroperoxide induced oxidative stress in rat hepatocytes. In an effort to throw more light on the mechanism mediating their hepatoprotective action, the effects of the newly synthesized compounds on the hepatocyte parameters related to cell membrane integrity and oxidative stress have been studied. DFT calculations in nonpolar and polar medium have been applied to predict the most probable mechanisms of free-radicals scavenging in comparison with those suggested for melatonin. The membrane permeability of the studied compounds has been characterized based on calculated physico-chemical properties such as polar surface area, molecular weight, number of rotatable bonds and number of hydrogen-bond acceptors and donors.

## 2. Materials and methods

Melting points (mp) have been determined using an Electrothermal AZ 9000 3MK4 apparatus and are uncorrected. IR spectra have been recorded on a Bruker spectrometer as potassium bromide discs and ATR. $^1$H and $^{13}$C NMR spectra have been recorded on a Bruker Avance II+ 250 MHz and a Bruker Avance II+ 600 MHz NMR instrument. The spectra are referred to the solvent signal. Chemical shifts are expressed in ppm and coupling constants in Hz. The precise assignment of the $^1$H and $^{13}$C NMR spectra has been accomplished by measurement of 2D homonuclear correlation (COSY), DEPT-135 and 2D inverse detected heteronuclear (C–H) correlation HSQC**.** The reactions have been monitored by thin layer chromatography performed on Merck pre-coated plates (silica gel. 60 $F_{254}$, 0.25 mm) and visualized by fluorescence quenching under UV light (254 nm).

The chemicals used in the pharmacological experiments were: pentobarbital sodium (Sanofi, France), HEPES (Sigma Aldrich, Germany), NaCl (Merck, Germany), KCl (Merck), D-glucose (Merck), $NaHCO_3$ (Merck), $KH_2PO_4$ (Scharlau Chemie SA, Spain), $CaCl_2 \cdot 2H_2O$ (Merck), $MgSO_4 \cdot 7H_2O$ (Fluka AG, Germany), collagenase from *Clostridium histolyticum* type IV (Sigma Aldrich), albumin, bovine serum fraction V, minimum 98% (Sigma Aldrich), EGTA (Sigma Aldrich), 2-thiobarbituric acid (4,6-dihydroxypyrimidine-2-thiol; TBA) (Sigma Aldrich), trichloroacetic acid (TCA) (Valerus, Bulgaria), 2,2′-dinitro-5,5′-dithiodibenzoic acid (DTNB) (Merck), lactate dehydrogenase (LDH) kit (Randox, UK), *tert*-butyl hydroperoxide (Sigma Aldrich), carbon tetrachloride (Merck).

### 2.1. Synthesis

#### 2.1.1. General procedure for preparation of compounds **16–45**

To a solution of the hydrazides of N,N′-disubstituted benzimidaozle-2-thiones (**11–15**) in absolute ethanol an o-, m- or p-substituted methoxy or fluorobenzaldehyde were added and the solution was refluxed for 2 h.

*2.1.1.1. 3,3′-(2-thioxo-1H-benzo[d]imidazole-1,3(2H)-diyl)bis(N′-(4-methoxybenzylidene) propanehydrazide) (**16**).* Yield 89%, Mp 230–232 °C, IR ($\nu_{max}$/cm$^{-1}$) 3205 (νN-H); 2947 ($\nu_{as}$ CH); 1650 ($\nu$ C=O) amide I; 1606 ($\nu$ C=N); 1560 (δ N–H); 1249 ($\nu_{as}$ C–O–C); 1211 ($\nu$ C=S); 833 (γ C–H) phenyl (p-)

$^1$H NMR (250 MHz, DMSO-$d_6$) δ: 11.31–11.33 (d, $J$ = 5.9 Hz, 1H, NH); 11.24–11.26 (d, $J$ = 4.9 Hz, 1H, NH); 8.03–8.04 (d, $J$ = 2.6 Hz, 1H, CH), 7.84–7.86 (d, $J$ = 4.2 Hz, 1H, CH), 7.59–7.62 (d, $J$ = 5.9 Hz, 2H, Ar–H),7.45–7.54 (m, 4H, Ar–H), 7.24–7.28 (m, 2H, Ar–H), 6.89–6.98 (m, 4H, Ar–H), 4.62–4.51 (m, 4H,$CH_2$), 3.77–3.80 (d, $J$ = 7.2 Hz, 6H, $CH_3$), 3.01–3.13 (m, 2H, $CH_2$), 2.70–2.79 (m, 2H, $CH_2$).

$^{13}$C NMR (75 MHz, DMSO-$d_6$) δ: 171.7, 168.1, 165.8, 160.5, 146.3, 143.1, 131.4, 128.6, 128.3, 126.7, 126.6, 122.7, 114.2, 109.6, 55.3, 30.6.

*2.1.1.2. 3,3′-(2-thioxo-1H-benzo[d]imidazole-1,3(2H)-diyl)bis(N′-(2-methoxybenzylidene) propanehydrazide) (**17**).* Yiled 87%, Mp 230–231 °C, IR ($\nu_{max}$/cm$^{-1}$) 3178 (νN-H); 2950 ($\nu_{as}$ CH); 1670 ($\nu$ C=O) amide I; 1606 ($\nu$ C=N); 1567 (δ N–H); 1215 ($\nu$ C=S); 753 (γ C–H) phenyl (o-)

$^1$H NMR (250 MHz, DMSO-$d_6$) δ: 11.45–11.48 (d, $J$ = 6.6 Hz, 1H, NH); 11.33–11.36 (d, $J$ = 6.3 Hz, 1H, NH); 8.44–8.45 (d, $J$ = 3.9 Hz, 1H, CH), 8.25–8.26 (d, $J$ = 4.7 Hz, 1H, CH), 7.76–7.79 (d, $J$ = 7.7 Hz, 2H, Ar–H), 7.44–7.52 (m, 2H, Ar–H), 7.33–7.43 (m, 2H, Ar–H), 7.22–7.27 (m, 2H, Ar–H), 7.02–7.09 (m, 2H, Ar–H), 7.88–7.99 (m, 2H, Ar–H), 4.52–4.62 (m, 4H,$CH_2$), 3.80–3.82 (d, $J$ = 5.5 Hz, 6H, $CH_3$), 3.04–3.14 (m, 2H, $CH_2$), 2.69–2.75 (m, 2H, $CH_2$).

$^{13}$C NMR (75 MHz, DMSO-$d_6$) δ: 171.8, 165.9, 157.7, 157.5138.9, 131.4, 131.2, 125.3, 122.7, 122.1, 120.7, 120.6, 111.7, 109.9, 55.7, 32.3, 30.6.

*2.1.1.3. 3,3′-(2-thioxo-1H-benzo[d]imidazole-1,3(2H)-diyl)bis(N′-(3-methylbenzylidene) propanehydrazide) (**18**).* Yield 73%, Mp 177–179 °C, IR ($\nu_{max}$/cm$^{-1}$) 3189 (νN-H); 2952 ($\nu_{as}$ CH); 1664 ($\nu$ C=O) amide I; 1613 ($\nu$ C=N); 1578 (δ N–H); 1254 ($\nu_{as}$ C–O–C); 1221 ($\nu$ C=S); 778, 687 (γ C–H) phenyl (m-)

$^1$H NMR (250 MHz, DMSO-$d_6$) δ: 11.45–11.48 (d, $J$ = 8.3 Hz, 1H, NH), 11.37–11.40 (d, $J$ = 7.4 Hz, 1H, NH); 8.07–8.08 (d, $J$ = 3.90 Hz, 1H, CH), 7.85–7.87 (d, $J$ = 5.17 Hz, 1H, CH), 7.42–7.57 (m, 2H, Ar–H), 7.30–7.38 (m, 1H, Ar–H), 7.22–7.28 (m, 4H, Ar–H), 7.10–7.17 (m, 2H, Ar–H), 6.99–7.01 (m, 2H, Ar–H), 4.49–4.62 (m, 4H,$CH_2$),

3.75–3.77 (d, $J = 3.4$ Hz, 6H, $CH_3$), 3.05–3.17 (m, 2H, $CH_2$), 2.63–2.81 (m, 2H, $CH_2$).

$^{13}$C NMR (75 MHz, DMSO-$d_6$) δ: 172.0, 168.1, 166.2, 159.5, 146.3, 143.1, 135.6, 135.4, 131.3, 129.8, 122.7, 119.9, 115.6, 111.5, 111.2, 109.5, 55.2, 32.3, 30.6.

*2.1.1.4. 3,3′-(2-thioxo-1H-benzo[d]imidazole-1,3(2H)-diyl)bis(N′-(4-fluorobenzylidene) propanehydrazide) (**19**).* Yield 91%, Mp 236–237 °C, IR ($\nu_{max}$/cm$^{-1}$) 3212 (νN-H); 2950 ($\nu_{as}$ CH); 1680, 1657 ($\nu$ C=O) amide I; 1604 ($\nu$ C=N); 1561 (δ N–H); 1213 ($\nu$ C=S); 1059 ($\nu$ C–F); 831 (γ C–H) phenyl (p-)

$^1$H NMR (250 MHz, DMSO-$d_6$) δ: 11.46–11.48 (d, $J = 5.8$ Hz, 1H, NH), 11.38–11.40 (d, $J = 5.3$ Hz, 1H, NH), 8.10–8.11 (d, $J = 2.5$ Hz, 1H, CH), 7.89–7.91 (d, $J = 4.2$ Hz, 1H, CH), 7.56–7.75 (m, 4H, Ar–H), 7.45–7.54 (m, 2H, Ar–H), 7.15–7.30 (m, Hz, 6H, Ar–H), 4.51–4.60 (m, 4H,$CH_2$), 3.05–3.15 (t, $J = 26.36$ Hz, 2H, $CH_2$), 2.72–2.78 (m, 2H, $CH_2$).

$^{13}$C NMR (75 MHz, DMSO-$d_6$) δ: 171.9, 168.1, 166.1, 145.2, 142.0, 131.3, 130.6, 129.2, 129.0, 128.7, 122.7, 115.8, 109.9, 111.2, 32.3, 30.5.

*2.1.1.5. 3,3′-(2-thioxo-1H-benzo[d]imidazole-1,3(2H)-diyl)bis(N′-(2-fluorobenzylidene) propanehydrazide) (**20**).* Yield 88%, Mp 251–253 °C, IR ($\nu_{max}$/cm$^{-1}$) 3248 (νN-H); 2956 ($\nu_{as}$ CH); 1669, 1658 ($\nu$ C=O) amide I; 1609 ($\nu$ C=N); 1548 (δ N–H); 1215 ($\nu$ C=S); 1043 ($\nu$ C–F); 762 (γ C–H) phenyl (o-)

$^1$H NMR (250 MHz, DMSO-$d_6$) δ: 11.60–11.63 (d, $J = 7.00$ Hz, 1H, NH), 11.48–11.50 (d, $J = 7.0$ Hz, 1H, NH), 8.31–8.33 (d, $J = 4.3$ Hz, 1H, CH), 8.09–8.12 (d, $J = 5.5$ Hz, 1H, CH), 7.68–7.89 (m, 2H, CH), 7.37–7.56 (m, 4H, Ar–H), 7.15–7.30 (m, 6H, Ar–H), 4.50–4.63 (m, 4H,$CH_2$), 3.06–3.16 (m, 2H, $CH_3$), 2.73–2.78 (m, 2H, $CH_2$).

$^{13}$C NMR (75 MHz, DMSO-$d_6$) δ: 172.1, 168.1, 166.2, 162.5, 136.0, 131.7, 131.5, 131.3, 126.1, 124.7, 122.7, 121.5, 121.4, 116.0, 115.7, 109.6, 30.5.

*2.1.1.6. 3,3′-(2-thioxo-1H-benzo[d]imidazole-1,3(2H)-diyl)bis(N′-(3-fluorobenzylidene) propanehydrazide) (**21**).* Yield 91%, Mp 236–238 °C, IR ($\nu_{max}$/cm$^{-1}$) 3185 (νN-H); 2974 ($\nu_{as}$ CH); 1665 ($\nu$ C=O) amide I; 1614 ($\nu$ C=N); 1583 (δ N–H); 1239 ($\nu$ C=S); 1049 ($\nu$ C–F); 781, 686 (γ C–H) phenyl (m-)

$^1$H NMR (250 MHz, DMSO-$d_6$) δ: 11.60–11.63 (d, $J = 7.0$ Hz, 1H, NH), 11.48–11.50 (d, $J = 7.0$ Hz, 1H, NH), 8.31–8.33 (d, $J = 4.2$ Hz, 1H, CH), 8.09–8.12 (d, $J = 5.5$ Hz, 1H, CH), 7.68–7.89 (m, 2H, Ar–H), 7.40–7.49 (m, 4H, Ar–H), 7.15–7.30 (m, 6H, Ar–H), 4.50–4.63 (m, 4H, $CH_2$), 3.06–3.16 (m, 4H, $CH_2$).

$^{13}$C NMR (63 MHz, DMSO-$d_6$) δ: 172.14, 168.11, 168.11, 166.31, 164.25, 160.37, 144.94, 141.85, 136.56, 131.33, 130.75, 123.16, 122.69, 116.59, 113.14, 112.74, 112.37, 109.95, 109.52, 32.41, 30.55.

*2.1.1.7. 3,3′-(5-methyl-2-thioxo-1H-benzo[d]imidazole-1,3(2H)-diyl) bis(N′-((E)-4-methoxybenzylidene)propanehydrazide) (**22**).* Yield 87%, Mp 242–244 °C, IR ($\nu_{max}$/cm$^{-1}$) 3207 (νN-H); 2945 ($\nu_{as}$ CH); 1653 ($\nu$ C=O) amide I; 1607 ($\nu$ C=N); 1560 (δ N–H); 1251 ($\nu_{as}$ C–O–C); 1214 ($\nu$ C=S); 832 (γ C–H) phenyl (p-)

$^1$H NMR (250 MHz, DMSO-$d_6$) δ: 11.26–11.35 (m, 2H, NH), 8.01–8.04 (m, 1H, CH), 7.82–7.88 (m, 1H, CH), 7.46–7.60 (m, 4H, Ar–H), 7.28–7.39 (m, 2H, Ar–H), 6.90–7.07 (m, 5H, Ar–H), 4.45–4.55 (m, 4H, $CH_2$), 3.75–3.79 (m, 6H, $CH_3$), 3.01–3.08 (m, 2H, $CH_2$), 2.68–2.74 (m, 2H, $CH_2$), 2.37–2.39 (d, $J = 7.0$ Hz, 3H, $CH_3$).

$^{13}$C NMR (63 MHz, DMSO-$d_6$) δ: 172.14, 168.11, 168.11, 166.31, 164.25, 164.25, 160.37, 144.94, 141.85, 136.56, 131.33, 130.75, 123.16, 122.69, 116.59, 113.14, 112.74, 112.37, 109.95, 109.52, 32.41, 30.55.

*2.1.1.8. 3,3′-(5-methyl-2-thioxo-1H-benzo[d]imidazole-1,3(2H)-diyl) bis(N′-((E)-2-methoxybenzylidene)propanehydrazide) (**23**).* Yield 75%, Mp 218–220 °C, IR ($\nu_{max}$/cm$^{-1}$) 3181 (νN-H); 2949 ($\nu_{as}$ CH); 1672 ($\nu$ C=O) amide I; 1607 ($\nu$ C=N); 1575 (δ N–H); 1250 ($\nu_{as}$ C–O–C); 1215 ($\nu$ C=S); 752 (γ C–H) phenyl (o-)

$^1$H NMR (600 MHz, DMSO-$d_6$) δ 11.35–11.47 (m, 2H, NH), 8.45–8.48 (m, 1H, CH), 8.25–8.29 (m, 1H, CH),7.63–7.79 (m, 2H, Ar–H), 7.28–7.43 (m, 4H, Ar–H), 6.88–7.10 (m, 5H, Ar–H), 4.49–4.59 (m, 4H, $CH_2$), 3.81–3.83 (d, $J = 4.18$ Hz, 6H, $CH_3$), 3.03–3.12 (m, 2H, $CH_2$), 2.71–2.74 (m, 2H, $CH_2$), 2.39–2.40 (d, $J = 3.1$ Hz, 3H, $CH_3$).

$^{13}$C NMR (63 MHz, DMSO-$d_6$) δ: 168.6, 167.7, 140.4, 131.7, 127.8, 126.0, 110.6, 114.4, 130.2, 130.75, 123.16, 122.69, 116.59, 113.14, 112.74, 112.37, 109.95, 109.52, 55.8, 55.6, 34.7.

*2.1.1.9. 3,3′-(5-methyl-2-thioxo-1H-benzo[d]imidazole-1,3(2H)-diyl) bis(N′-((E)-3-methoxybenzylidene)propanehydrazide) (**24**).* Yield 83%, Mp 212–215 °C, IR ($\nu_{max}$/cm$_{-1}$) 3180 (νN-H); 2955 ($\nu_{as}$ CH); 1665 ($\nu$ C=O) amide I; 1598 ($\nu$ C= N); 1580 (δ N–H); 1266 ($\nu_{as}$ C–O–C); 1230 ($\nu$ C=S); 732, 686 (γ C–H) phenyl (m-)

$^1$H NMR (600 MHz, DMSO-$d_6$) δ 11.37–11.47 (m, 2H, NH), 8.07–8.10 (m, 1H, CH), 7.86–7.89 (m, 1H, CH), 6.94–7.44 (m, 11H, Ar–H), 4.49–4.56 (m, 4H, $CH_2$), 3.75–3.80 (m, 6H, CH3), 3.04–3.14 (m, 2H, $CH_2$), 2.70–2.76 (m, 2H, CH2), 2.38–2.40 (d, $J = 3.1$ Hz, 3H, $CH_3$).

$^{13}$C NMR (150 MHz, DMSO-$d_6$) δ: 172.48, 168.10, 166.63, 159.90, 146.71, 143.54, 136.07, 135.87, 132.71, 130.35, 129.89, 124.07, 120.39, 119.71, 119.65, 116.01, 111.99, 110.14, 55.61, 55.58, 31.03, 21.53.

*2.1.1.10. 3,3′-(5-methyl-2-thioxo-1H-benzo[d]imidazole-1,3(2H)-diyl)bis(N′-((E)-4-fluorobenzylidene)propanehydrazide) (**25**).* Yield 87%, Mp 242–244 °C IR ($\nu_{max}$/cm$^{-1}$) 3184 (νN-H); 2967 ($\nu_{as}$ CH); 1668 ($\nu$ C=O) amide I; 1602 ($\nu$ C= N); 1560 (δ N–H); 1215 ($\nu$ C=S); 1052 ($\nu$ C–F); 835 (γ C–H) phenyl (p-)

$^1$H NMR (600 MHz, DMSO-$d_6$) δ: 11.40–11.49 (m, 2H, NH), 8.08–8.11 (m, 1H, CH), 7.88–7.90 (m, 1H, CH), 7.59–7.72 (m, 4H, Ar–H), 7.06–7.35 (m, 7H, Ar–H), 4.45–4.56 (m, 4H, $CH_2$), 4.63–4.36 (m, 3H, $CH_3$), 3.03–3.10 (m, 4H, $CH_2$), 2.70–2.75 (m, 2H, $CH_2$), 2.37–2.38 (d, $J = 6.5$ Hz, 3H, $CH_3$).

$^{13}$C NMR (150 MHz, DMSO-$d_6$) δ: 172.44, 168.23, 166.60, 164.12, 162.48, 145.69, 142.48, 131.08, 129.92, 129.68, 129.33, 124.11, 116.23, 116.13, 110.26, 109.81, 31.01, 21.55.

*2.1.1.11. 3,3′-(5-methyl-2-thioxo-1H-benzo[d]imidazole-1,3(2H)-diyl) bis(N′-((E)-2-fluorobenzylidene)propanehydrazide) (**26**).* Yield 84%, Mp 242–244 °C, IR ($\nu_{max}$/cm$^{-1}$) 3183 (νN-H); 2953 ($\nu_{as}$ CH); 1672 ($\nu$ C=O) amide I; 1607 ($\nu$ C=N); 1568 (δ N–H); 1210 ($\nu$ C=S); 1050 ($\nu$ C–F); 756 (γ C–H) phenyl (o-)

$^1$H NMR (600 MHz, DMSO-$d_6$) δ: 11.50–11.62 (m, 2H, NH), 8.30–8.34 (m, 1H, CH), 8.09–8.13 (m, 1H, NH), 7.16–7.49 (m, 8H, Ar–H), 7.06–7.09 (m, 1H, Ar–H), 4.45–4.56 (m, 4H, $CH_2$), 3.04–3.11 (m, 4H, $CH_2$), 2.37–2.38 (d, $J = 3.9$ Hz, 3H, $CH_3$).

$^{13}$C NMR (150 MHz, DMSO-$d_6$) δ: 172.57, 168.12, 166.54, 161.87, 160.07, 152.38, 136.26, 131.96, 129.91, 126.59, 125.24, 124.11, 110.19, 56.49, 32.86, 31.01, 21.55, 19.02.

*2.1.1.12. 3,3′-(5-methyl-2-thioxo-1H-benzo[d]imidazole-1,3(2H)-diyl)bis(N′-((E)-3-fluorobenzylidene)propanehydrazide) (**27**).* Yield 84%, Mp 280–283 °C, IR ($\nu_{max}$/cm$^{-1}$) 3192 (νN-H); 2922 ($\nu_{as}$ CH); 1678 ($\nu$ C=O) amide I; 1607 ($\nu$ C=N); 1577 (δ N–H); 1214 ($\nu$ C=S); 1052 ($\nu$ C–F); 783, 685 (γ C–H) phenyl (m-)

$^1$H NMR (600 MHz, DMSO-$d_6$) δ: 11.48–11.59 (m, 2H, NH), 8.08–8.11 (m, 1H, CH), 7.87–7.90 (m, 1H, CH), 7.17–7.50 (m, 10H, Ar–H), 7.04–7.07 (m, 1H, Ar–H), 4.44–4.56 (m, 4H, $CH_2$), 3.03–3.11 (m, 2H, $CH_2$), 2.71–2.76 (m, 2H, $CH_2$), 2.37 (s, 3H, $CH_3$).

$^{13}$C NMR (63 MHz, DMSO-$d_6$) δ: 172.0, 167.8, 166.2, 162.5, 158.5, 139.1, 135.9, 132.3, 131.6, 131.5, 129.4, 126.1, 124.7, 123.6, 121.6, 115.9, 115.7, 109.7, 109.3, 32.4, 30.5, 21.0.

*2.1.1.13. 3,3′-(5-nitro-2-thioxo-1H-benzo[d]imidazole-1,3(2H)-diyl) bis(N′-((E)-4-methoxybenzylidene)propanehydrazide)* (***28***). Yield 84%, Mp 268-171 °C, IR ($\nu_{max}$/cm$^{-1}$) 3162 (νN-H); 2967 ($\nu_{as}$ CH); 1650 ($\nu$ C═O) amide I; 1602 ($\nu$ C= N); 1575 (δ N–H); 1508 ($\nu_{as}$ $NO_2$); 1322 ($\nu_s$ $NO_2$); 1251 ($\nu_{as}$ C–O–C); 1214 ($\nu$ C═S); 832 (γ C–H) phenyl (p-)

$^1$H NMR (600 MHz, DMSO-$d_6$) δ: 11.69–11.34 (m, 2H, NH), 8.60–8.63 (m, 1H, CH), 8.52–8.56 (m, 1H, CH), 7.78–8.20 (m, 6H, Ar–H), 7.43–7.59 (m,4, Ar–H), 6.96–6.98 (m,1H, Ar–H), 4.63–4.72 (m, 4H, $CH_2$), 3.76–3.78 (m, 2H, $CH_3$), 3.22–3.26 (m, 2H, $CH_2$), 2.81–2.84 (m, 2H, $CH_2$).

$^{13}$C NMR (63 MHz, DMSO-$d_6$) δ: 171.1, 168.6, 167.7, 162.9, 158.8, 157.4, 145.5, 144.2, 140.3, 130.2, 129.7, 126.0, 124.6, 123.5, 112.8, 112.3, 55.8, 55.6, 34.2, 33.8.

*2.1.1.14. 3,3′-(5-nitro-2-thioxo-1H-benzo[d]imidazole-1,3(2H)-diyl) bis(N′-(2-methoxybenzylidene)propanehydrazide)* (***29***). Yield 84%, Mp 232–234 °C, IR ($\nu_{max}$/cm$^{-1}$) 3193 (νN-H); 2946 ($\nu_{as}$ CH); 1676 ($\nu$ C═O) amide I; 1607 ($\nu$ C═N); 1580 (δ N–H); 1525 ($\nu_{as}$ $NO_2$); 1339 ($\nu_s$ $NO_2$); 1250 ($\nu_{as}$ C–O–C); 1214 ($\nu$ C═S); 753 (γ C–H) phenyl (o-)

$^1$H NMR (600 MHz, DMSO-$d_6$) δ: 11.37–11.42 (m, 2H, NH), 8.56–8.60 (m, 1H, CH), 8.52–8.54 (m, 1H, CH), 8.25–8.15 (m, 1H, Ar–H), 7.55–8.21 (m, 7H, Ar–H), 7.33–7.40 (m, Hz, 2H, Ar–H), 7.03–7.07 (m, 2H, Ar–H), 4.63–4.72 (m, 4H, $CH_2$), 3.79–3.81 (d, $J$ = 7.9 Hz, 6H, $CH_3$), 3.23–3.27 (m, 2H, $CH_2$), 2.80–2.84 (m, 2H, $CH_2$).

$^{13}$C NMR (63 MHz, DMSO-$d_6$) δ: 172.2, 169.7, 168.6, 161.9, 159.8, 156.7, 146.5, 145.7, 142.3, 131.4, 128.6, 127.4, 123.6, 122.7, 111.9, 111.4, 56.3, 55.9, 35.3, 33.8.

*2.1.1.15. 3,3′-(5-nitro-2-thioxo-1H-benzo[d]imidazole-1,3(2H)-diyl) bis(N′-((E)-3-methoxybenzylidene)propanehydrazide)* (***30***). Yield 82%, Mp 188–190 °C, IR ($\nu_{max}$/cm$^{-1}$) 3184 ($\nu$ N–H); 2962 ($\nu_{as}$ CH); 1667 ($\nu$ C═O) amide I; 1596 ($\nu$ C═N); 1580 (δ N–H); 1509 ($\nu_{as}$ $NO_2$); 1344 ($\nu_s$ $NO_2$); 1218 ($\nu$ C═S); 736, 687 (γ C–H) phenyl (m-)

$^1$H NMR (600 MHz, DMSO-$d_6$) δ: 11.59–11.24 (m, 2H, NH), 8.53–8.61 (m, 2H, CH), 8.20–8.02 (m, 2H, Ar–H), 7.77–7.97 (m, 3H, Ar–H), 6.95–7.34 (m, 8H, Ar–H), 4.67–4.76 (m, 4H, $CH_2$), 3.76–3.79 (d, $J$ = 8.2, Hz, 6H, $CH_3$), 3.26–3.31 (m, 2H, $CH_2$), 2.85–2.90 (m, 2H, $CH_2$).

$^{13}$C NMR (63 MHz, DMSO-$d_6$) δ: 170.9, 168.3, 167.9, 162.1, 158.4, 155.4, 147.3, 144.9, 143.4, 132.3, 129.7, 128.5, 122.7, 121.7, 112.6, 111.3, 55.6, 55.3, 35.7, 34.3.

*2.1.1.16. 3,3′-(5-nitro-2-thioxo-1H-benzo[d]imidazole-1,3(2H)-diyl) bis(N′-((E)-4-fluorobenzylidene)propanehydrazide)* (***31***). Yield 82%, Mp 155–157 °C, IR ($\nu_{max}$/cm$^{-1}$) 3183 (νN-H); 2972 ($\nu_{as}$ CH); 1676, 1644 ($\nu$ C═O) amide I; 1616 ($\nu$ C═N); 1585 (δ N–H); 1510 ($\nu_{as}$ $NO_2$); 1348 ($\nu_s$ $NO_2$); 1216 ($\nu$ C═S); 1056 ($\nu$ C–F); 837 (γ C–H) phenyl (p-)

$^1$H NMR (600 MHz, DMSO-$d_6$) δ: 11.42–11.43 (d, $J$ = 7.2 Hz, 2H, NH), 8.76–8.77 (d, $J$ = 2.2 Hz, 2H, CH), 8.08–8.04 (m, 1H, Ar–H), 7.78–7.87 (m, 3H, Ar–H), 7.69–7.71 (m, 4H, Ar–H), 7.17–7.21 (m, 4H, Ar–H), 4.70–4.72 (m, 4H, $CH_2$), 3.25–3.27 (m, 2H, $CH_2$), 2.84–2.85 (m, 2H, $CH_2$).

$^{13}$C NMR (63 MHz, DMSO-$d_6$) δ: 172.2, 170.2, 169.8, 161.8, 159.5, 156.4, 148.4, 145.3, 142.1, 133.6, 128.4, 127.7, 123.6, 122.7, 112.4, 112.0, 35.5, 35.0.

*2.1.1.17. 3,3′-(5-nitro-2-thioxo-1H-benzo[d]imidazole-1,3(2H)-diyl) bis(N′-((E)-2-fluorobenzylidene)propanehydrazide)* (***32***). Yield 82%, Mp 163–165 °C, IR ($\nu_{max}$/cm$^{-1}$) 3200 (νN-H); 2953 ($\nu_{as}$ CH); 1677 ($\nu$ C═O) amide I; 1607 ($\nu$ C= N); 1585 (δ N–H); 1521 ($\nu_{as}$ $NO_2$); 1348 ($\nu_s$ $NO_2$); 1220 ($\nu$ C═S); 1062 ($\nu$ C–F); 762 (γ C–H) phenyl (o-)

$^1$H NMR (250 MHz, DMSO-$d_6$) δ: 11.52–11.58 (m, 2H, NH), 8.76–8.77 (d, $J$ = 2.1 Hz, 1H, CH), 8.48–8.49 (d, $J$ = 2.2 Hz, 1H, CH), 7.68–8.22 (m, 7H, Ar–H), 7.18–7.45 (m, 4H, Ar–H), 4.65–4.76 (m, 4H, $CH_2$), 3.28–3.32 (m, 2H, $CH_2$), 2.85–2.90 (m, 2H, $CH_2$).

$^{13}$C NMR (63 MHz, DMSO-$d_6$) δ: 171.9, 171.2, 168.7, 162.7, 158.4, 155.2, 147.8, 144.4, 140.7, 134.8, 129.1, 128.5, 123.8, 123.0, 112.7, 111.9, 36.8, 36.1.

*2.1.1.18. 3,3′-(5-nitro-2-thioxo-1H-benzo[d]imidazole-1,3(2H)-diyl) bis(N′-((E)-3-fluorobenzylidene)propanehydrazide)* (***33***). Yield 82%, Mp 208–210 °C, IR ($\nu_{max}$/cm$^{-1}$) 3204 (νN-H); 2955 ($\nu_{as}$ CH); 1681 ($\nu$ C═O) amide I; 1609 ($\nu$ C= N); 1578 (δ N–H); 1520 ($\nu_{as}$ $NO_2$); 1347 ($\nu_s$ $NO_2$); 1219 ($\nu$ C═S); 1045 ($\nu$ C–F); 786, 683 (γ C–H) phenyl (m-)

$^1$H NMR (250 MHz, DMSO-$d_6$) δ: 11.49–11.52 (d, $J$ = 6.9 Hz, 2H, NH), 8.77–8.78 (d, $J$ = 2.2 Hz 1H, CH), 8.47–8.48 (d, $J$ = 2.1, 1H, CH), 8.05–8.24 (m, 3H, Ar–H), 7.17–7,50 (m, 8H, Ar–H), 4.65–4.75 (m, 4H, $CH_2$), 3.26–3.35 (m, 2H, $CH_2$), 2.86–2.91 (m, 2H, $CH_2$).

$^{13}$C NMR (63 MHz, DMSO-$d_6$) δ: 172.1, 168.8, 166.4, 162.6, 158.0, 156.1, 148.1, 143.7, 141.6, 135.9, 130.2, 129.4, 122.6, 123.2, 112.5, 112.1, 35.2, 34.9.

*2.1.1.19. 3,3′-(5-chloro-2-thioxo-1H-benzo[d]imidazole-1,3(2H)-diyl) bis(N′-((E)-4-methoxybenzylidene)propanehydrazide)* (***34***). Yield 86%, Mp 119–222 °C, IR ($\nu_{max}$/cm$^{-1}$) 3181 (νN-H); 2954 ($\nu_{as}$ CH); 1665 ($\nu$ C═O) amide I; 1605 ($\nu$ C═N); 1573 (δ N–H); 1252 ($\nu_{as}$ C–O–C); 1222 ($\nu$ C═S); 832 (γ C–H) phenyl (p-)

$^1$H NMR (600 MHz, DMSO-$d_6$) δ: 11.25–11.34 (m, 2H, NH), 8.00–8.03 (m, 1H, CH), 7.16–7.84 (m, 1H, CH), 7.43–7.61 (m, 6H, Ar–H), 7.27–7.30 (m, 1H, Ar–H), 6.89–6.98 (m, 4H, Ar–H), 4.44–4.57 (m, 4H, $CH_2$), 3.75–3.78 (m, 6H, $CH_3$), 3.02–3.10 (m, 2H, $CH_2$), 2.69–2.76 (m, 2H, $CH_2$).

$^{13}$C NMR (151 MHz, DMSO-$d_6$) δ: 171.3, 168.5, 164.4, 157.3, 155.8, 140.1, 137.2, 131.7, 130.5, 128.8, 126.7, 125.5, 123.8, 121.2, 111.3, 110.1, 55.2, 55.0, 32.8, 30.4.

*2.1.1.20. 3,3′-(5-chloro-2-thioxo-1H-benzo[d]imidazole-1,3(2H)-diyl) bis(N′-((E)-2-methoxybenzylidene)propanehydrazide)* (***35***). Yield 78%, Mp 239–241 °C, IR ($\nu_{max}$/cm$^{-1}$) 3178 (νN-H); 2949 ($\nu_{as}$ CH); 1672 ($\nu$ C═O) amide I; 1606 ($\nu$ C═N); 1574 (δ N–H); 1249 ($\nu_{as}$ C–O–C); 1220 ($\nu$ C═S); 751 (γ C–H) phenyl (o-)

$^1$H NMR (600 MHz, DMSO-$d_6$) δ: 11.34–11.47 (m, 2H, NH), 8.41–8.45 (m, 1H, CH), 8.21–8.27 (m, 1H, CH), 7.59–7.78 (m, 3H, Ar–H), 7.45–7.54 (m, 1H, Ar–H), 7.24–7.40 (m, 3H, Ar–H), 6.88–7.07 (m 4H, Ar–H), 4.43–4.56 (m, 4H, $CH_2$), 3.79–3.82 (m, 6H, $CH_3$), 3.04–3.12 (m, 2H, $CH_2$), 2.69–2.75 (m, 2H, $CH_2$).

$^{13}$C NMR (151 MHz, DMSO-$d_6$) δ: 172.61, 172.29, 169.43, 169.38, 166.31, 158.10, 157.93, 142.31, 139.33, 132.82, 131.98, 131.62, 130.85, 127.80, 125.69, 122.95, 122.51, 121.17, 121.10, 112.10, 56.04, 32.68, 30.98, 30.94.

*2.1.1.21. 3,3′-(5-chloro-2-thioxo-1H-benzo[d]imidazole-1,3(2H)-diyl) bis(N′-((E)-3-methoxybenzylidene)propanehydrazide)* (***36***). Yield 83%, Mp 185–188 °C, IR ($\nu_{max}$/cm$^{-1}$) 3183 (νN-H); 2964 ($\nu_{as}$ CH); 1669 ($\nu$ C═O) amide I; 1611 ($\nu$ C═N); 1580 (δ N–H); 1265 ($\nu_{as}$ C–O–C); 1218 ($\nu$ C═S); 780,687 (γ C–H) phenyl (m-)

$^1$H NMR (250 MHz, DMSO-$d_6$) δ: 11.36–11.47 (m, 2H, NH), 8.06–8.09 (t, $J$ = 4.3 Hz, 1H, CH), 7.85–7.86 (d, $J$ = 4.0 Hz, 1H, CH), 7.58–7.71 (m, 1H, Ar–H), 7.43–7.54 (m, 1H, Ar–H), 7.20–7.35 (m, 4H, Ar–H), 7.11–7.14 (m, 3H, Ar–H), 6.93–7.02 (m, 2H, Ar–H), 4.46–4.60 (m, 4H, $CH_2$), 3.76–3.85 (m, 6H, $CH_3$), 3.08–3.13 (m, 4H, $CH_2$), 2.71–2.79 (m, 4H, $CH_2$).

$^{13}$C NMR (151 MHz, DMSO-$d_6$) δ: 173.4, 169.5, 168.2, 157.2, 156.7, 141.5, 137.7, 133.4, 132.5, 129.4, 127.6, 124.2, 121.7, 120.3, 112.2, 112.1, 56.9, 56.1, 31.4, 30.8.

*2.1.1.22. 3,3′-(5-chloro-2-thioxo-1H-benzo[d]imidazole-1,3(2H)-diyl) bis(N′-((E)-4-fluorobenzylidene)propanehydrazide)* (***37***). Yield 81%,

Mp 196–198 °C, IR ($\nu_{max}$/cm$^{-1}$) 3181 (νN-H); 2972 ($\nu_{as}$ CH); 1672 ($\nu$ C=O) amide I; 1602 ($\nu$ C= N); 1580 (δ N–H); 1212 ($\nu$ C=S); 1049 ($\nu$ C–F); 834 (γ C–H) phenyl (p-)

$^1$H NMR (250 MHz, DMSO-$d_6$) δ: 11.49–11.25 (m, 2H, NH), 7.99 (dd, $J$ = 52.3, 3.2 Hz, 2H, CH), 7.78–7.65 (m, 2H, Ar–H), 7.62 (d, $J$ = 2.1 Hz, 2H, Ar–H), 7.59–7.44 (m, 2H, Ar–H), 7.30 (t, $J$ = 3.2 Hz, 1H, Ar–H), 7.28–7.13 (m, 4H, Ar–H), 4.72–4.30 (m, 4H, $CH_2$), 3.23–2.61 (m, 4H, $CH_2$).

$^{13}$C NMR (151 MHz, DMSO-$d_6$) δ: 172.4, 169.4, 166.5, 162.4, 145.7, 142.4, 132.8, 131.0, 130.8, 129.6, 129.3, 123.0, 116.4, 116.2, 116.1, 111.3, 110.3, 32.6, 30.9.

*2.1.1.23. 3,3′-(5-chloro-2-thioxo-1H-benzo[d]imidazole-1,3(2H)-diyl) bis(N′-((E)-2-fluorobenzylidene)propanehydrazide) (**38**).* Yield 83%, Mp 278–280 °C, IR ($\nu_{max}$/cm$^{-1}$) 3185 (νN-H); 2957 ($\nu_{as}$ CH); 1672 ($\nu$ C=O) amide I; 1610 ($\nu$ C= N); 1590 (δ N–H); 1216 ($\nu$ C=S); 1092 ($\nu$ C–F); 758 (γ C–H) phenyl (o-)

$^1$H NMR (250 MHz, DMSO-$d_6$) δ: 11.77–11.32 (m, 2H, NH), 8.33 (t, $J$ = 4.1 Hz, 1H, CH), 8.12 (t, $J$ = 3.8 Hz, 1H, CH), 7.92–7.75 (m, 1H, Ar–H), 7.75–7.59 (m, 2H, Ar–H), 7.58–7.49 (m, 1H, Ar–H), 7.49–7.34 (m, 2H, Ar–H), 7.31 (t, $J$ = 4.9 Hz, 1H, Ar–H), 7.25 (d, $J$ = 8.3 Hz, 2H, Ar–H), 7.17 (d, $J$ = 7.9 Hz, 2H, Ar–H), 4.86–4.12 (m, 4H, CH2), 3.18–2.57 (m, 4H, CH2).

$^{13}$C NMR (151 MHz, DMSO-$d_6$) δ: 172.2, 168.9, 165.7, 163.2, 143.6, 141.4, 131.2, 130.0, 129.8, 128.4, 128.2, 122.0, 117.7, 117.2, 116.9, 110.3, 110.2, 31.6, 30.9.

*2.1.1.24. 3,3′-(5-chloro-2-thioxo-1H-benzo[d]imidazole-1,3(2H)-diyl) bis(N′-((E)-3-fluorobenzylidene)propanehydrazide) (**39**).* Yield 78%, Mp 243–246 °C, IR ($\nu_{max}$/cm$^{-1}$) 3178 (νN-H); 2962 ($\nu_{as}$ CH); 1666 ($\nu$ C=O) amide I; 1609 ($\nu$ C=N); 1579 (δ N–H); 1214 ($\nu$ C=S); 1049 ($\nu$ C–F); 775, 683 (γ C–H) phenyl (m-)

$^1$H NMR (250 MHz, DMSO-$d_6$) δ: 11.46–11.57 (m, 2H, NH), 8.10–8.11 (d, $J$ = 3.7 Hz, 1H, CH), 7.88–7.90 (d, $J$ = 3.4 Hz, 1H, CH), 7.60–7.71 (m, 1H, Ar–H), 7.35–7.54 (m, 7H, Ar–H), 7.16–7.32 (m, 3H, Ar–H), 4.45–4.61 (m, 4H, $CH_2$), 3.05–3.13 (m, 2H, $CH_2$), 2.73–2.78 (m, 2H, $CH_2$).

$^{13}$C NMR (151 MHz, DMSO-$d_6$) δ: 171.6, 169.8, 167.4, 161.4, 146.8, 143.6, 131.9, 131.4, 130.1, 128.6, 127.4, 122.3, 118.5, 117.2, 117.1, 112.5, 111.3, 33.9, 31.8.

*2.1.1.25. 3,3′-(5-benzoyl-2-thioxo-1H-benzo[d]imidazole-1,3(2H)-diyl)bis(N′-((E)-4-methoxybenzylidene)propanehydrazide) (**40**).* Yield 85%, Mp 191–192 °C, IR ($\nu_{max}$/cm$^{-1}$) 3246 (νN-H); 2956 ($\nu_{as}$ CH); 2837 ($\nu_s$ CH); 1678 ($\nu$ C=O) amide I; 1645 ($\nu$ C=O) benzoyl; 1606 ($\nu$ C=N); 1575 (δ N–H); 1252 ($\nu_{as}$ C–O–C); 1217 ($\nu$ C=S); 830, 698 (γ C–H) phenyl.

$^1$H NMR (250 MHz, DMSO-$d_6$) δ: 11.30–11.48 (m, 2H, NH), 8.41–8.45 (t, $J$ = 4.9 Hz, 1H, CH), 8.18–8.23 (t, $J$ = 4.9 Hz, 1H, CH), 7.75–7.98 (m, 4H, Ar–H), 7.51–7.70 (m, 6H, Ar–H), 7.32–7.39 (m, 2H, Ar–H), 6.87–7.10 (m, 6H, Ar–H), 4.52–4.63 (m, 4H, $CH_2$), 3.78–3.82 (m, 6H, $CH_3$), 3.11–3.19 (m, 2H, $CH_2$), 2.74–2.79 (m, 2H, $CH_2$).

$^{13}$C NMR (63 MHz, DMSO-$d_6$) δ: 172.2, 166.6, 161.5, 145.2, 135.8, 133.6, 132.7, 131.4, 131.2, 125.3, 129.7, 129.3, 129.0, 125.3, 123.2, 121.0, 115.1, 54.7, 54.5, 30.5.

*2.1.1.26. 3,3′-(5-benzoyl-2-thioxo-1H-benzo[d]imidazole-1,3(2H)-diyl)bis(N′-((E)-2-methoxybenzylidene)propanehydrazide) (**41**).* Yield 83%, Mp 185–186 °C, IR ($\nu_{max}$/cm$^{-1}$) 3185 (νN-H); 2921 ($\nu_{as}$ CH); 2849 ($\nu_s$ CH); 1669 ($\nu$ C=O) amide I; 1648 ($\nu$ C=O) benzoyl; 1603 ($\nu$ C=N); 1574 (δ N–H); 1250 ($\nu_{as}$ C–O–C); 1225 ($\nu$ C=S); 753 (γ C–H) phenyl (o-)

$^1$H NMR (250 MHz, DMSO-$d_6$) δ 11.21–11.34 (m, 2H, NH), 8.48–8.56 (m, 2H, CH), 7.75–7.84 (m, 3H, CH), 7.45–7.69 (m, 9H, Ar–H), 6.89–7.08 (m, 4H, Ar–H), 4.53–4.65 (m, 4H, $CH_2$), 3.76–3.80 (m, 6H, $CH_3$), 3.06–3.17 (m, 2H, $CH_2$), 2.75–2.90 (m, 2H, $CH_2$).

$^{13}$C NMR (63 MHz, DMSO-$d_6$) δ 171.7, 165.7, 160.4, 146.1, 134.9, 134.6, 132.5, 131.6, 131.3, 129.6, 128.6, 128.4, 128.1, 126.5, 124.5, 124.0, 114.0, 55.2, 55.1, 30.5.

*2.1.1.27. 3,3′-(5-benzoyl-2-thioxo-1H-benzo[d]imidazole-1,3(2H)-diyl)bis(N′-((E)-3-methoxybenzylidene)propanehydrazide) (**42**).* Yield 87%, Mp 190-186 °C, IR ($\nu_{max}$/cm$^{-1}$) 3192 (νN-H); 2958 ($\nu_{as}$ CH); 2851 ($\nu_s$ CH); 1671 ($\nu$ C=O) amide I; 1653 ($\nu$ C=O) benzoyl; 1612 ($\nu$ C=N); 1576 (δ N–H); 1264 ($\nu_{as}$ C–O–C); 1220 ($\nu$ C=S); 783, 688 (γ C–H) phenyl (m-)

$^1$H NMR (600 MHz, DMSO-$d_6$) δ: 11.30–11.48 (m, 2H, NH), 8.07–7.94 (m, 1H, CH), 7.38–7.67 (m, 5H, Ar–H), 7.08–7.33 (m, 8H, Ar–H), 6.89–6.98 (m, 3H, Ar–H), 4.45–4.65 (m, 4H, $CH_2$), 3.71–3.75 (m, 6H, $CH_3$), 3.08–3.18 (m, 2H, $CH_2$), 2.73–2.82 (m, 2H, $CH_2$).

$^{13}$C NMR (63 MHz, DMSO-$d_6$) δ: 172.1, 167.7, 161.3, 144.9, 134.9, 132.5, 131.9, 131.2, 130.7, 128.4, 127.9, 126.3, 125.8, 124.1, 121.0, 118.0, 116.1, 55.9, 55.7.

*2.1.1.28. 3,3′-(5-benzoyl-2-thioxo-1H-benzo[d]imidazole-1,3(2H)-diyl)bis(N′-((E)-4-fluorobenzylidene)propanehydrazide) (**43**).* Yield 88%, Mp 240–241 °C, IR ($\nu_{max}$/cm$^{-1}$) 3194 (νN-H); 2957 ($\nu_{as}$ CH); 2833 ($\nu_s$ CH); 1670 ($\nu$ C=O) amide I; 1653 ($\nu$ C=O) beznoyl; 1610 ($\nu$ C=N); 1576 (δ N–H); 1230 ($\nu$ C=S); 1041 ($\nu$ C–F); 783, 688 (γ C–H) phenyl.

$^1$H NMR (600 MHz, DMSO-$d_6$) δ 11.31–11.49 (m, 2H, NH), 7.79–8.05 (m, 2H, CH), 7.73–7.77 (m, 2H, Ar–H), 7.61–7.67 (m, 2H, Ar–H), 7.51–7.59 (m, 2H, Ar–H), 7.24–7.33 (m, 2H, Ar–H), 7.07–7.21 (m, 4H, Ar–H), 6.91–6.98 (m, 2H, Ar–H), 4.45–4.64 (m, 4H, $CH_2$), 3.72–3.77 (m, 3H, $CH_3$), 3.07–3.18 (m, 2H, $CH_2$), 2.72–2.83 (m, 2H, $CH_2$).

$^{13}$C NMR (151 MHz, DMSO-$d_6$) δ 196.5, 172.8, 169.5, 160.4, 158.7, 153.0, 141.1, 139.3, 137.8, 136.0, 134.2, 131.0, 129.7, 128.4, 126.9, 125.3, 124.0, 117.8, 112.5, 111.4, 30.9, 30.4.

*2.1.1.29. 3,3′-(5-benzoyl-2-thioxo-1H-benzo[d]imidazole-1,3(2H)-diyl)bis(N′-(2-fluorobenzylidene)propanehydrazide) (**44**).* Yield 81%, Mp 255–257 °C, IR ($\nu_{max}$/cm$^{-1}$) 3185 (νN-H); 2951 ($\nu_{as}$ CH); 2864 ($\nu_s$ CH); 1677 ($\nu$ C=O) amide I; 1657 ($\nu$ C=O) benzoyl; 1606 ($\nu$ C= N); 1576 (δ N–H); 1232 ($\nu$ C=S); 1048 ($\nu$ C–F); 760 (γ C–H) phenyl.

$^1$H NMR (600 MHz, DMSO-$d_6$) δ: 11.48–11.64 (m, 2H, NH), 8.27–8.31 (m, 1H, CH), 8.04–8.10 (m, 1H, CH), 7.51–7.77 (m, 10H, Ar–H), 7.39–7.48 (m, 2H, Ar–H), 7.15–7.28 (m, 4H, Ar–H), 4.49–4.65 (m, 4H, $CH_2$), 3.10–3.17 (m, 2H, $CH_2$), 2.76–2.84 (m, 2H, $CH_2$).

$^{13}$C NMR (151 MHz, DMSO-$d_6$) δ: 195.43, 172.55, 170.43, 161.84, 160.27, 154.02, 139.71, 137.83, 136.48, 135.04, 133.00, 132.03, 130.13, 128.96, 126.54, 125.78, 125.09, 116.29, 111.92, 110.33, 31.93, 30.96.

*2.1.1.30. 3,3′-(5-benzoyl-2-thioxo-1H-benzo[d]imidazole-1,3(2H)-diyl)bis(N′-((E)-3-fluorobenzylidene)propanehydrazide) (**45**).* Yield 85%, Mp 268-267 °C, IR ($\nu_{max}$/cm$^{-1}$) 3187 (νN-H); 2958 ($\nu_{as}$ CH); 2857 ($\nu_s$ CH); 1677 ($\nu$ C=O) amide I; 1654 ($\nu$ C=O) benzoyl; 1607 ($\nu$ C=N); 1576 (δ N–H); 1223 ($\nu$ C=S); 1049 ($\nu$ C–F); 783 (γ C–H) phenyl (m-)

$^1$H NMR (600 MHz, DMSO-$d_6$) δ: 11.62–11.34 (m, 2H, NH), 7.91–7.80 (m, 2H, CH), 7.74 (d, $J$ = 7.7 Hz, 1H, Ar–H), 7.68–7.60 (m, 2H, Ar–H), 7.55 (dd, $J$ = 13.1, 5.5 Hz, 2H, Ar–H), 7.50–7.43 (m, 2H, Ar–H), 7.41–7.37 (m, 2H, Ar–H), 7.36–7.32 (m, 2H, Ar–H), 7.26–7.11 (m, 3H, Ar–H), 4.77–4.35 (m, 4H, $CH_2$), 3.16 (t, $J$ = 7.0 Hz, 2H, $CH_2$), 3.10 (dd, $J$ = 12.8, 6.7 Hz, 2H, $CH_2$).

$^{13}$C NMR (151 MHz, DMSO-$d_6$) δ: 194.3, 172.5, 171.1, 162.0, 158.9,

155.0, 138.1, 135.8, 134.8, 134.2, 133.3, 132.7, 131.3, 129.6, 127.4, 126.8, 125.9, 117.9, 112.0, 111.3, 32.9, 31.2.

### 2.2. Evaluation of hepatotoxicity and hepatoprotective activity on in vitro model of tert-BuOOH induced oxidative stress

#### 2.2.1. Experimental design

*2.2.1.1. Isolation and incubation of hepatocytes.* Rats were anesthetized with sodium pentobarbital (0.2 ml/100 g). An optimized *in situ* liver perfusion using less reagents and shorter time of cell isolation was performed. The method provided a higher amount live and metabolically active hepatocytes [18].

After portal catheterization, the liver was perfused with HEPES buffer (pH = 7.85) + 0.6 mM EDTA (pH = 7.85), followed by clean HEPES buffer (pH = 7.85) and finally HEPES buffer containing collagenase type IV (50 mg/200 ml) and 7 mM $CaCl_2$ (pH = 7.85). The liver was excised, minced into small pieces, and hepatocytes were dispersed in Krebs-Ringer-bicarbonate (KRB) buffer (pH = 7.35) + 1% bovine serum albumin.

Cells were counted under the microscope and the viability was assessed by Trypan blue exclusion (0.05%) [19]. Initial viability averaged 89%. Cells were diluted with KRB to make a suspension of about $3 \times 10^6$ hepatocytes/ml. Incubations were carried out in flasks containing 3 ml of the cell suspension (i.e. $9 \times 10^6$ hepatocytes) and were performed in a 5% $CO_2$ + 95% $O_2$ atmosphere.

*2.2.1.2. Cell incubation.* Cells were incubated with 250 μM of the tested compounds and 75 μM *tert*-butyl hydroperoxide [20,21].

#### 2.2.2. Biochemical assays

*2.2.2.1. Lactate dehydrogenase (LDH) release.* After incubation, the hepatocytes were centrifuged for 4 min at 500 rpm and the supernatant was used for measuring LDH release spectrophotometrically by LDH kit [22].

*2.2.2.2. Reduced glutathione (GSH) depletion.* At the end of the incubation isolated rat hepatocytes were centrifuged (at 4 °C) and the pellet was used for evaluating the level of intracellular GSH. It was assessed by measuring non-protein sulfhydryls after precipitation of proteins with trichloroacetic acid (TCA), followed by measurement of thiols in the supernatant with DTN. The absorbance was measured at 412 nm [19].

*2.2.2.3. Malondialdehyde (MDA) assay.* After incubation, 1 ml from hepatocyte suspension was taken and added to 0.67 ml of 20% (w/v) TCA. After centrifugation, 1 ml of the supernatant was added to 0.33 ml of 0.67% (w/v) 2-thiobarbituric acid (TBA) and heated at 100 °C for 30 min. The absorbance was measured at 535 nm, and the amount of TBA-reactants was calculated using a molar extinction coefficient of MDA $1.56 \times 10^5\ M^{-1}cm^{-1}$ [19].

#### 2.2.3. Statistical analysis

For statistical analysis of the data we used the MEDCALC statistical program. Results are expressed as mean ± SEM for 6 experiments. The significance of the data was assessed using the nonparametric Mann–Whitney test. A level of $P < 0.05$ was considered significant. Three parallel samples were used.

### 2.3. Evaluation of the protection effect against oxidative damage using in vitro model systems

#### 2.3.1. Determination of the protection effect in the lipid containing model system

Colorimetric method was used for the quantitative determination of the thiobarbituric acid reactive substances (TBARS) [23]. The extent of the observed oxidative damage has been presented as percentage of the untreated control sample and has been named "molecular damage". All samples were prepared in phosphate saline buffer, pH 7.4, with concentration of the oxidisable substrate (lecithin) 1 mg/ml. The peroxidation was induced by the addition of $FeCl_2$ with concentration of 0.1 mmol/L. In the control sample the tested compounds were omitted. The samples were incubated at 37 °C for 30 min. Then 0.5 ml of 2.8% trichloroacetic acid and 0.5 ml of thiobarbituric acid were added. The mixture was heated at 100 °C using a water bath for 20 min and centrifuged at 3000 rpm for 20 min. The absorbance of the samples was measured at 532 nm.

#### 2.3.2. Determination of the protective effect using the deoxyribose modified test

The tested compounds and the 2- deoxyribose [0.5 mmol/L] were diluted in phosphate saline buffer ($K_2HPO_4/KH_2PO_4$, pH 7.4) [24]. The deoxyribose damage was induced by the addition of $FeCl_2$ with concentration of 0.1 mmol/L. The mixture was incubated at 37 °C for 30 min and then 0.5 ml of 2.8% trichloroacetic acid and 0.5 ml of thiobarbituric acid were added. The samples were heated at 100 °C using a water bath and their absorbance was measured at 532 nm. The antioxidant activity of the tested compounds was determined using the formula:

$$AOA\% = ((A_{control} - A_{sample})/A_{control})) \times 100$$

### 2.4. Computational details

All theoretical calculations were performed using the Gaussian 09 package [25] of programs. Geometry and vibrational frequencies of species studied were performed by an analytical gradient technique without any symmetry constraint. All the results were obtained using the density functional theory (DFT), employing the B3LYP (Becke's three-parameter non-local exchange [26] and Lee et al. correlation [27] potentials). In order to find the preferred geometry of 1,3-dibstituted benzimidazole-2-thiones in isolated state, a large number of probable conformations were constructed and optimized at B3LYP/6-31+G* level of theory. For every structure the stationary points found on the molecular potential energy hypersurfaces were characterized using standard analytical harmonic vibrational analysis. The absence of imaginary frequencies, as well as of negative eigenvalues of the second-derivative matrix, confirmed that the stationary points correspond to minima on the potential energy hypersurface.

Dissociation enthalpy (BDE) and ionization potential (IP) of the studied compounds were calculated according to the equations reported in Ref. [28]. All reaction enthalpies were calculated at 298 K. Solvation enthalpies of proton $H(H^+)$, and electron, $H(e^-)$, in organic solvents were calculated using IEF-PCM DFT/B3LYP/6-31+G*. Solvation enthalpy of electron, $H(e^-)$ was determined as:

$$H(e^-)_{solv} = H(DMSO^{\bullet})_{solv} - H(DMSO)_{solv} - H(e^-)_{gas},$$

where $H(e^-)_{gas}$ is 3.145 kJ $mol^{-1}$ following the procedure already applied on similar studies [29,30].

The following free radicals were included in the study: •OR/ROH and •OOR/ROOH, where R = (Z)-4-hydroperoxyhex-2-ene.

The lipid radicals were modelled for comparison according to the same computational Scheme.

Relaxed IP was calculated as the difference between the energy of the optimized radical cation and the optimized neutral molecule [31].

## 3. Results and discussion

### 3.1. Chemistry

Compounds **1**–**15** were synthesized as previously reported [12]. The new hydrazone derivatives **16**–**45** were synthesized by refluxing the hydrazide compounds **11**–**15** in absolute ethanol with the respective o-, m- or p-methoxy and o-, m- or p-fluoro substituted benzaldehydes. In this way, from the five precursor hydrazides, the following groups of hydrazone derivatives were obtained (Table 1): group I (**16**–**21**, no substituent in the benzimidazole ring); group II (**22**–**27**, 5-$CH_3$); group III (**28**–**33**, 5-$NO_2$); group IV (**34**–**39**, 5-Cl); and group V (**39**–**45**, 5-$COC_6H_2$) (Scheme 1).

DFT B3LYP/6-31+G* optimization showed that the benzimidazole-2-thione fragment is essentially flat, while the side chains are very flexible and may occupy several conformations producing conformers with energy differences within 0.8–2.5 kJ $mol^{-1}$ (conformers **16C1**–**16C4** in Fig. 1, relatives energies are listed in Table 1S in Supplementary material). Molecular structure with *trans* orientation of the side chains (facing the opposite sides of the benzimidazole plane) and carbonyl groups pointing towards the benzimidazole ring is the preferred one due to stabilization through C–H···S and C–H···O short contacts (conformer **16C1** in Fig. 1). Similar interactions have been found for esters **6** and **10** in crystal state [12]. Extended conformations of the side chains where stabilization through the above-mentioned short contacts does not occur are less favorable (conformers **16C3** and **16C4** in Fig. 1). Formation of an intramolecular hydrogen bond between the H-atom from the azomethine group and the carbonyl group also contributes to the stabilization as evidenced by the energy difference of 7.80 kJ $mol^{-1}$ between conformers **16C1a** and **16C1b** (Table 1S in Supplementary material). The small energy differences between conformers **16C1**–**16C4**, implies that all these forms might be present in solution. This assumption is confirmed by the registered multiple sets of resonances in the $^1$H NMR spectra of compounds **16**–**45** following the same proportion as the Boltzmann population ration calculated on the basis of the energy differences between the conformers.

**Table 1**
Substituents in the hydrazone benzimidazole-2-thione derivatives.

| Compound | $R_1$ | $R_2$ | Compound | $R_1$ | $R_2$ |
|---|---|---|---|---|---|
| **16** | H | p-$OCH_3$ | **31** | $NO_2$ | p-F |
| **17** | H | *o*-$OCH_3$ | **32** | $NO_2$ | o-F |
| **18** | H | m-$OCH_3$ | **33** | $NO_2$ | m-F |
| **19** | H | p-F | **34** | Cl | p-$OCH_3$ |
| **20** | H | o-F | **35** | Cl | *o*-$OCH_3$ |
| **21** | H | m-F | **36** | Cl | m-$OCH_3$ |
| **22** | $CH_3$ | p-$OCH_3$ | **37** | Cl | p-F |
| **23** | $CH_3$ | *o*-$OCH_3$ | **38** | Cl | o-F |
| **24** | $CH_3$ | m-$OCH_3$ | **39** | Cl | m-F |
| **25** | $CH_3$ | p-F | **40** | $COC_6H_5$ | p-$OCH_3$ |
| **26** | $CH_3$ | o-F | **41** | $COC_6H_5$ | *o*-$OCH_3$ |
| **27** | $CH_3$ | m-F | **42** | $COC_6H_5$ | m-$OCH_3$ |
| **28** | $NO_2$ | p-$OCH_3$ | **43** | $COC_6H_5$ | p-F |
| **29** | $NO_2$ | *o*-$OCH_3$ | **44** | $COC_6H_5$ | o-F |
| **30** | $NO_2$ | m-$OCH_3$ | **45** | $COC_6H_5$ | m-F |

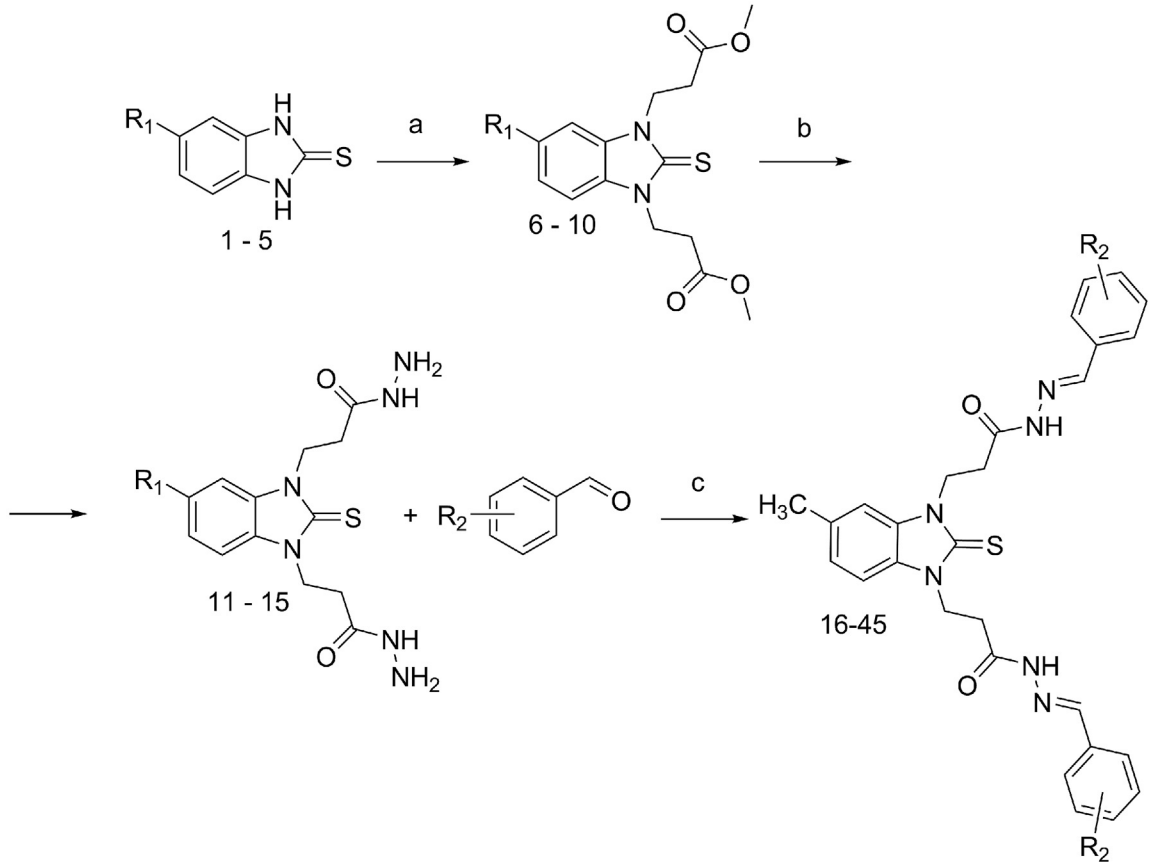


**Scheme 1.** Synthesis of the studied benzimidazole-2-thione compounds. Reagents and conditions: a) methyl acrylate, DMF, refluxing; b) hydrazine hydrate, ethanol solution, refluxing; c) substituted benzaldehyde, ethanol, refluxing. $R_1$ and $R_2$ are listed in Table 1.

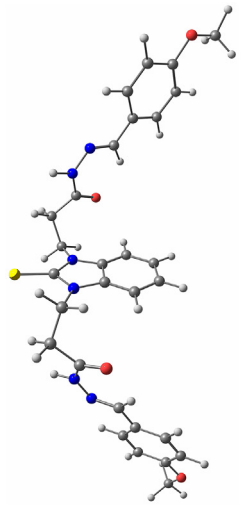

16C1 - trans

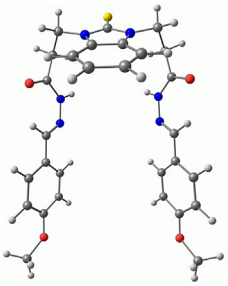

16C2 -cis

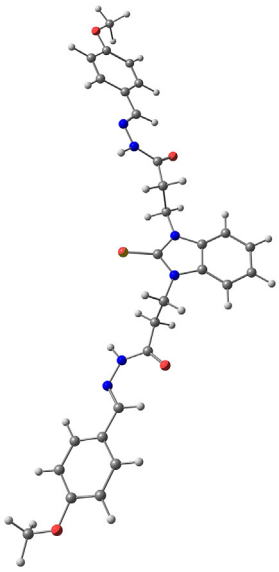

16C3 - trans

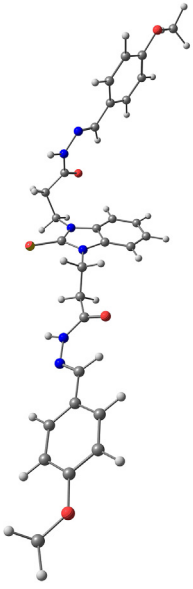

16C4 -trans

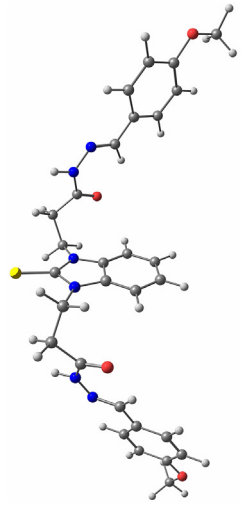

16C1a - Z

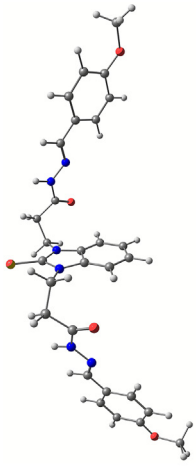

16C1b - E

### 3.2. Pharmacology

#### 3.2.1. Toxicological potential study of benzimidazole-2-thiones 16–45 on isolated rat hepatocytes

A study on the effect of benzimidazole-2-thiones **16**–**45** on the functional-metabolic status of isolated rat hepatocytes has been carried out in order to evaluate their toxicological potential. Isolated rat hepatocytes are convenient well-controlled biological model *in vitro* systems recommended by the European Centre for the Validation of Alternative Methods (ECVAM) as alternative methods reducing the use of laboratory animals [32,33]. The compounds were tested on isolated hepatocytes from male Wistar rats, prepared by two-stepped collagenase perfusion.

The effect of the compounds on the functional-metabolic status of the hepatocytes has been assessed by monitoring the cell viability; intracellular lactate dehydrogenase (LDH), hepatic glutathione (GSH) depletion and production of malondialdehyde (MDA). All of them are being used as biomarkers revealing different aspects of the oxidative stress injuries in the living cells and have a potential role in predicting the progression of oxidative stress associated pathophysiological conditions and their response to therapies.

The studied compounds have affected the functional-metabolic status of isolated rat hepatocytes to a different extent (Table 2). The compounds have been administered alone, in concentration 250 μM [34]. All the observed effects have been compared to a control group of non-treated hepatocytes.

The data in Table 2 indicate that from all of the studied hydrazones, the unsubstituted **16**–**21** administered alone, have revealed the lowest cytotoxic effects on isolated rat hepatocytes. Previously it was found that 5-benzoyl derivatives revealed the lowest toxicological potential within series of analogous esters and hydrazides [12]. In the group of the hydrazones unsubstituted in position 5 of the beznimidazole cycle, **16**–**18** possessing a methoxyphenyl group have exhibited lower cytotoxicity than the ones with a fluorophenyl substituents. The last observation is valid throughout the examined groups because all of the fluorophenyl substituted hydrazones have demonstrated higher unfavourable effects compared to the ones containing methoxyphenyl. Compounds **16**–**18** have decreased cell viability by 13–15% and increased the LDH leakage by 168–199% which is statistically significant. The compounds from group I have shown no statistically significant toxic effect on the level of the reduced glutathione. The MDA production has increased by 71–77%. The other two groups of hydrazones substituted in position 5 of the benzimidazole ring with methyl (**24**–**27**) and benzoyl groups (**40**–**45**) also have exhibited relatively low hepatotoxicity. In the groups of the hydrazones substituted with a nitro group (**28**–**33**) and a chlorine atom (**34**–**39**), the most unfavorably affecting the functional-metabolic parameters compounds have been found where the chloro derivatives have the highest toxicological potential which is in accordance with our previous results.

From the studies parameters parameters, administered alone, the compounds from group I (**16**–**21**) were the least cytotoxic compared to the other four groups; after that came group V (**40**–**45**) followed by group II (**22**–**27**) and the more cytotoxic compounds from group III (**28**–**33**). The most cytotoxic group was group IV (**34**–**39**).

The toxicity increased in the following manner: **H** < **($C_6H_5CO$)** < **$CH_3$** < **$NO_2$** < **Cl**.

**Fig. 1.** Optimized geometry of conformers **16C1**–**16C4** with different conformations of the side chains and **16C1a, b** as a result from rotation around the N–N bond.

**Table 2**
Effects of the tested compounds in concentration of 250 μM on the parameters characterizing the functional-metabolic status of isolated rat hepatocytes.

| Group | Compound | Cell viability, % | LDH, μmol/min/$10^6$ | GSH, nmol/$10^6$ | MDA, nmol/$10^6$ |
|---|---|---|---|---|---|
| | control | 82 ± 1.5 | 0.112 ± 0.01 | 19 ± 1.2 | 0.052 ± 0.01 |
| I | 16 | 70 ± 2.5* | 0.220 ± 0.01** | 18 ± 2.5 | 0.089 ± 0.01* |
| | 17 | 71 ± 2.3* | 0.225 ± 0.01** | 18 ± 2.2 | 0.091 ± 0.01* |
| | 18 | 71 ± 2.4* | 0.231 ± 0.01** | 18 ± 2.6 | 0.092 ± 0.01* |
| | 19 | 65 ± 2.5* | 0.300 ± 0.01*** | 16 ± 1.5 | 0.110 ± 0.01* |
| | 20 | 65 ± 2.1* | 0.320 ± 0.01*** | 16 ± 2.5 | 0.122 ± 0.01*** |
| | 21 | 63 ± 2.2* | 0.335 ± 0.01*** | 16 ± 2.1 | 0.125 ± 0.01** |
| II | 22 | 66 ± 1.1*** | 0.210 ± 0.02*** | 16 ± 1.7** | 0.211 ± 0.01*** |
| | 23 | 67 ± 1.1*** | 0.216 ± 0.02*** | 17 ± 1.2* | 0.217 ± 0.01*** |
| | 24 | 68 ± 1.2*** | 0.203 ± 0.01*** | 16 ± 2.5* | 0.214 ± 0.02*** |
| | 25 | 60 ± 1.6*** | 0.297 ± 0.01*** | 11 ± 1.1*** | 0.238 ± 0.02*** |
| | 26 | 61 ± 1.1*** | 0.281 ± 0.01*** | 10 ± 2.1*** | 0.238 ± 0.01*** |
| | 27 | 61 ± 1.1*** | 0.300 ± 0.01*** | 9 ± 1.5*** | 0.241 ± 0.01*** |
| III | 28 | 56 ± 1.5*** | 0.359 ± 0.01*** | 14 ± 1.5 | 0.227 ± 0.01*** |
| | 29 | 57 ± 2.1*** | 0.354 ± 0.01*** | 15 ± 1.2 | 0.227 ± 0.01*** |
| | 30 | 57 ± 2.1*** | 0.361 ± 0.01*** | 16 ± 2.5** | 0.228 ± 0.01*** |
| | 31 | 50 ± 1.5*** | 0.456 ± 0.01*** | 10 ± 1.7* | 0.348 ± 0.01*** |
| | 32 | 53 ± 2.6*** | 0.470 ± 0.01*** | 10 ± 1.7*** | 0.332 ± 0.01*** |
| | 33 | 51 ± 1.7*** | 0.469 ± 0.01*** | 9 ± 2.5*** | 0.328 ± 0.01*** |
| IV | 34 | 53 ± 2.1*** | 0.410 ± 0.02*** | 13 ± 1.7** | 0.111 ± 0.01** |
| | 35 | 51 ± 2.1** | 0.416 ± 0.02*** | 15 ± 1.2* | 0.117 ± 0.01** |
| | 36 | 51 ± 3.2** | 0.403 ± 0.01*** | 15 ± 2.5* | 0.114 ± 0.02** |
| | 37 | 47 ± 2.6*** | 0.497 ± 0.01*** | 11 ± 1.1*** | 0.138 ± 0.02* |
| | 38 | 47 ± 2.1** | 0.481 ± 0.01*** | 10 ± 2.1*** | 0.138 ± 0.01*** |
| | 39 | 46 ± 2.1** | 0.500 ± 0.01*** | 9 ± 1.5*** | 0.141 ± 0.01*** |
| V | 40 | 66 ± 1.5** | 0.259 ± 0.01*** | 16 ± 1.5 | 0.107 ± 0.01* |
| | 41 | 67 ± 2.1* | 0.254 ± 0.01*** | 17 ± 1.2 | 0.107 ± 0.01* |
| | 42 | 67 ± 2.1* | 0.261 ± 0.01*** | 18 ± 2.5 | 0.110 ± 0.01** |
| | 43 | 60 ± 1.5*** | 0.356 ± 0.01*** | 14 ± 1.7* | 0.128 ± 0.01** |
| | 44 | 63 ± 2.6* | 0.370 ± 0.01*** | 13 ± 1.7** | 0.132 ± 0.01*** |
| | 45 | 61 ± 1.7** | 0.369 ± 0.01*** | 14 ± 2.5* | 0.128± 0.01*** |

*P < 0.05; **P < 0.01; ***P < 0.001 vs control (non-treated hepatocytes).

*3.2.2. Evaluation of hepatoprotective activity in tert-butyl hydroperoxide-induced oxidative stress*

Nine hydrazones (**16**–**18**, **22**–**24** and **40**–**42**) which revealed the lowest cytotoxic effects on isolated rat hepatocytes from all the groups were selected and investigated for possible hepatoprotective and antioxidant activity in a model of *tert*-butyl hydroperoxide (tert-BuOOH)-induced oxidative stress.

Two mechanisms for tert-BuOOH action have been proposed: depletion of GSH cellular stores and oxidation of functionally important SH groups on mitochondrial enzymes, and/or changes of mitochondrial membrane integrity induced by peroxidation of membrane lipids [35]. Tert-BuOOH releases free radicals through one-electron oxidation to a peroxyl radical in the absence of NADPH or one-electron reduction to an alkoxyl radical in the presence of NADPH in microsomal suspension, and β-scission to methyl radical in isolated mitochondria and intact cells. All these radicals cause lipid peroxidation.

Administered alone, in concentration 75 μM, *tert*-butyl hydroperoxide has shown statistically significant cytotoxic effects on isolated rat hepatocytes – decreased cell viability and GSH level by 79%, and increased LDH leakage and MDA production by 492% and 476%, respectively. Quercetin in this model has preserved cell viability and GSH level – by 262% and 300%, respectively; and decreased LDH leakage and MDA production – by 54% and 79%, respectively, compared to the toxic agent (tert-BuOOH).

In combination with *tert*-butyl hydroperoxide, **16** has preserved cell viability by 233% ($p < 0.001$), **17** – by 257% ($p < 0.001$), **18** – by 243% ($p < 0.001$), **22** – by 181% ($p < 0.01$), **23** – by 186% ($p < 0.01$), **24** – by 162% ($p < 0.01$), **40** – by 233% ($p < 0.001$), **41** – by 214% ($p < 0.001$) and **42** – by 262% ($p < 0.001$), compared to the toxic agent. Effects have been compared with Quercetin (Figs. 2–5).

On this parameter, **22**–**24** have revealed statistically significant weaker cytoprotective effects, compared to those of Quercetin. All the others: **16**–**18** and **40**–**42** have shown cytoprotective effects similar to those of Quercetin.

In combination with *tert*-butyl hydroperoxide, **16** and **18** have decreased LDH leakage by 52% ($p < 0.001$), **17** – by 53% ($p < 0.001$), **22** – by 50% ($p < 0.001$), **23** – by 47% ($p < 0.001$), 24 – by 48% ($p < 0.001$), **40** and **42** – by 49% ($p < 0.01$) and **41** – by 51% ($p < 0.01$), compared to the toxic agent. On this parameter, all compounds have revealed statistically significant protective effects similar to those of Quercetin.

In combination with *tert*-butyl hydroperoxide, **16** has preserved GSH level with 281% ($p < 0.001$), **17** – with 305% ($p < 0.001$), **18** – with 290% ($p < 0.001$), **22** – with 52% ($p < 0.01$), **23** – with 124% ($p < 0.01$), **24** – with 100% ($p < 0.01$), **40** and **42** – with 252% ($p < 0.01$), **41** – with 300% ($p < 0.001$), compared to toxic agent. On this parameter, **22**, **23** and **24** have revealed statistically significant weaker protective effects, compared to those of Quercetin. All the others: **16**, **17**, **18**, **40**, **41** and **42** have shown similar protective effects to those of Quercetin.

In combination with *tert*-butyl hydroperoxide, **16** and **18** have decreased MDA production by 78% ($p < 0.001$), **17** – by 79% ($p < 0.001$), **22** – by 13% ($p < 0.01$), **23** – by 18% ($p < 0.01$), **24** – by 15% ($p < 0.01$), **40** and **42** – by 74% ($p < 0.001$) and **41** – by 78% ($p < 0.001$), compared to toxic the agent. On this parameter, **22**–**24** have revealed statistically significant weaker antioxidant effects, compared to those of Quercetin. All the others: **16**–**18** and **40**–**42** have shown similar antioxidant effects to those of Quercetin.

The cytoprotective effects of the studied compounds on tert-BuOOH-induced oxidative stress could be attributed to their activity as scavengers of ROS and influence on metabolism of *tert*-butyl hydroperoxide. As a result, the compounds have been able to reduce the lipid peroxidation, upregulate the GSH levels and protect the cell membrane integrity in the rat hepatocytes.

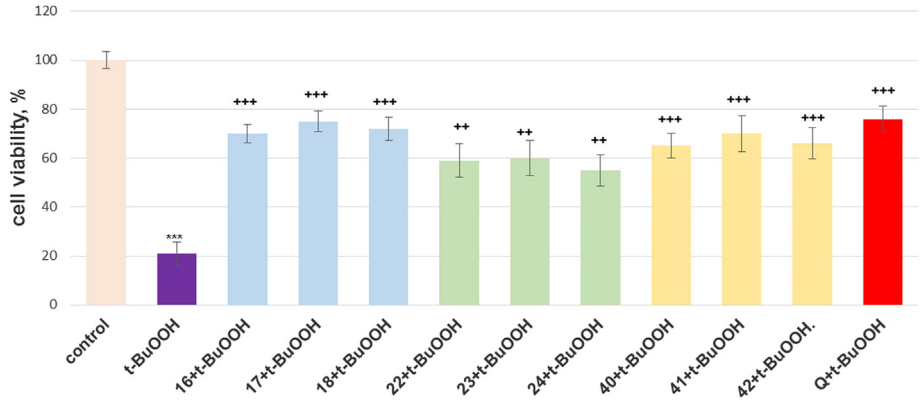


**Fig. 2.** Effects of 250 μM **16**–**18**, **22**–**24**, **40**–**42**, and Quercetin in *tert*-butyl hydroperoxide (75 μM)-induced oxidative stress on cell viability of isolated rat hepatocytes; $^{***}P < 0.001$ – vs control (non-treated hepatocytes); $^{++}$ $P < 0.01$; $^{+++}$ $P < 0.001$ – vs *tert*-butyl hydroperoxide.

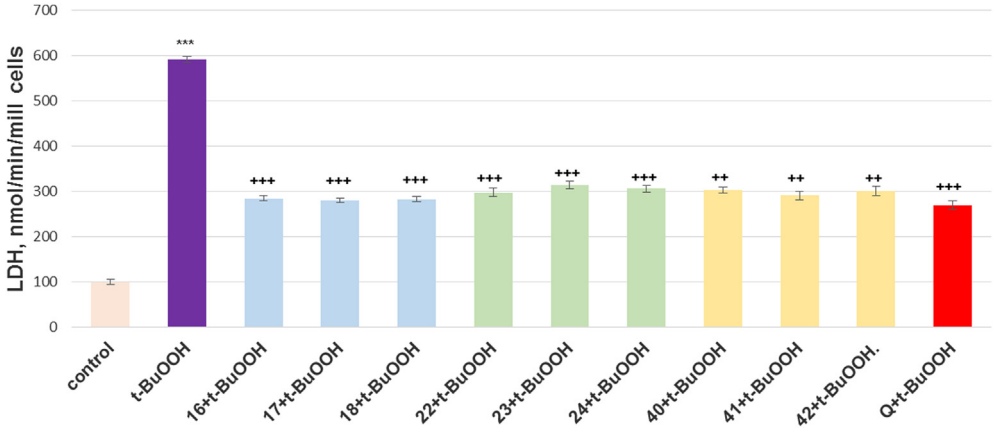


**Fig. 3.** Effects of 250 μM **16**–**18**, **22**–**24**, **40**–**42** and Quercetin in *tert*-butyl hydroperoxide (75 μM)-induced oxidative stress on LDH leakage in isolated rat hepatocytes; $^{***}P < 0.001$ – vs control (non-treated hepatocytes); $^{++}$ $P < 0.01$; $^{+++}$ $P < 0.001$ – vs *tert*-butyl hydroperoxide.

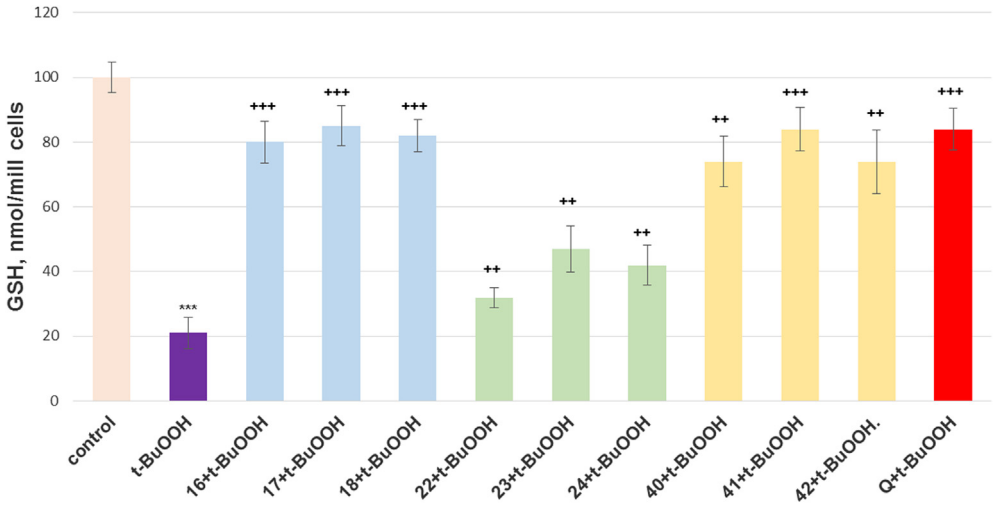


**Fig. 4.** Effects of 250 μM **16**–**18**, **22**–**24**, **40**–**42** and Quercetin in *tert*-butyl hydroperoxide (75 μM)-induced oxidative stress on GSH level in isolated rat hepatocytes; $^{***}P < 0.001$ – vs control (non-treated hepatocytes); $^{++}$ $P < 0.01$; $^{+++}$ $P < 0.001$ – vs *tert*-butyl hydroperoxide.

### *3.2.3. Evaluation of the protective effect against oxidative damage of biologically relevant molecules using in vitro model systems*

The revealed hepatoprotective effect of the tested hydrazones and the measured oxidative stress biomarkers in presence of these compounds suggests that they might be capable of preserving/protecting the basic cellular components from oxidative damage. Given the complexity of the pathophysiological mechanism of liver cells injuries associated with different diseases the evaluation of

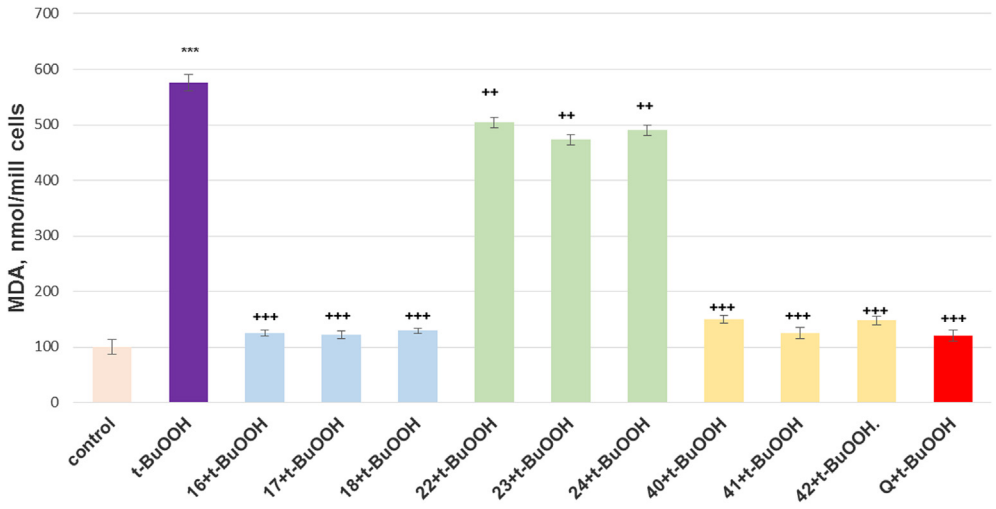


**Fig. 5.** Effects of 250 μM **16**–**18**, **22**–**24**, **40**–**42** and Quercetin in *tert*-butyl hydroperoxide (75 μM)-induced oxidative stress on MDA production in isolated rat hepatocytes; $^{***}P < 0.001$ – vs control (non-treated hepatocytes); $^{++}$ $P < 0.01$; $^{+++}$ $P < 0.001$ – vs *tert*-butyl hydroperoxide.

the possible oxidative stress processes and the capability of new effective hepatoprotectors to inhibit them is of biomedical, clinical, and pharmacological relevance. Transition metal induced oxidation of biologically relevant molecules is an important marker for oxidative stress. The evaluation of the protective effect of new designed compounds on this process is obligatory in the rating of the candidate compounds and the revealing of their optimal structural. Due to this fact the preliminary evaluation of the antioxidant activity of the tested hydrazones includes evaluation of their protection effect against iron induced oxidative damage in classic model systems containing basic biologically relevant molecules – lecithin and deoxyribose.

The lecithin containing model systems have been used to estimate the possible protection effect of the studied compounds against peroxidation of membrane lipid components which is associated with decrease in membrane fluidity, changes in its physicochemical properties and alteration of the biological function of its proteins. Another biologically important molecule which is the main target of free-radical induced degradation is DNA. Its structural damage is associated with changes of its sugar (deoxyribose) which induces strand breaking and formation of terminal fragmented sugar residues.

The conducted experiments in the lecithin containing model system have revealed that all the compounds inhibit the formation of thiobarbituric acid reactive substances (TBARS). The bars corresponding to the hydrazone containing samples are lower compared to the ones of the controls - which proves that the tested compounds have the capability to prevent the Fe(II) induced lipid peroxidation in this model system (Fig. 6). The % of molecular damage varies from 53.12% (compound **22**) to 68.92% (compound **41**). Compounds **17**, **22**, **23** and **24** have turned out to be the most potent ones. The observed molecular damage in the samples containing the most potent four hydrazones is approximately 2.5 and 2.9 times higher compared to the one in the mixtures with the reference antioxidants – Trolox and Quercetin.

For evaluation of the protection effect of the tested hydrazones on deoxyribose molecules a modified version of the Hallo well method for determination of the rate constant of interaction with hydroxyl radical has been used. In the initial assay a Fenton system is used for hydroxyl radicals initiated deoxyribose damage. In the simplified version of the assay we have used, the ascorbic acid and the hydrogen peroxide have been omitted from the reaction

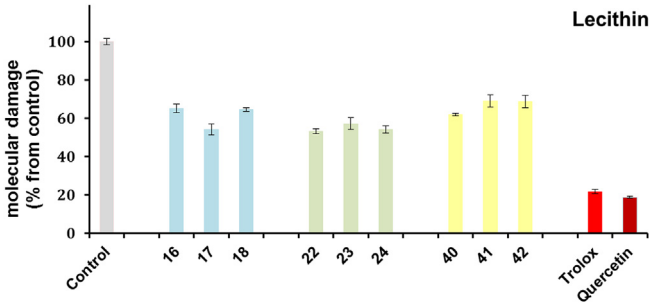


**Fig. 6.** Effect of **16**–**18**, **22**–**24**, **40**–**42** [90 μmol $L^{-1}$] on *in vitro* Fe(II) induced oxidative damage in the lecithin containing model system. Trolox and Quercetin at the same concentration have been used as reference compounds.

mixture. The possible mechanism of structural damages of the deoxyribose molecules includes autoxidation of the Fe(II) ions by $O_2$, generation of a superoxide anion radical and direct degradation of deoxyribose by the generated during the reaction $Fe^{3+}$ [36].

The tested compounds have exhibited diverse effects in the model system of iron induced deoxyribose damage (Fig. 7). The measured absorbances of the samples containing compounds **16**, **18**, **23** and **24** ($Abs_{16} = 0.303 \pm 0.013$, $Abs_{18} = 0.295 \pm 0.010$; $Abs_{23} = 0.279 \pm 0.015$; $Abs_{24} = 0.284 \pm 0.011$) compared to the one of the control samples ($Abs_{control\ 16\text{-}18} = 0.314 \pm 0.009$; $Abs_{control\ 22\text{-}24}$; $Abs_{control\ 40\text{-}42} = 0.272 \pm 0.010$) suggest negligibly low impact of these derivatives on the TBARS content.

The addition of compound **17** leads to statistically significant decrease of the absorbance ($Abs_{17} = 0.278 \pm 0.010$) indicating decreased TBARS content and possible protection effect against Fe(II) induced deoxyribose damage. Despite its relatively low effect the observed AOA = 11.56% results are comparable with those of the reference Trolox (AOA = 17.86). In the presence of the rest of the compounds we have observed different extent of increase of the absorbance of the samples compared to the control ones, which correlates with elevated TBARS content.

From the data obtained from the evaluation of the protection effect against oxidative damage of the lipid containing model system and the deoxyribose test we can conclude that the tested hydrazones exhibit variable behavior during Fe(II) oxidative damage depending on the used oxidisable substrate (lipid versus

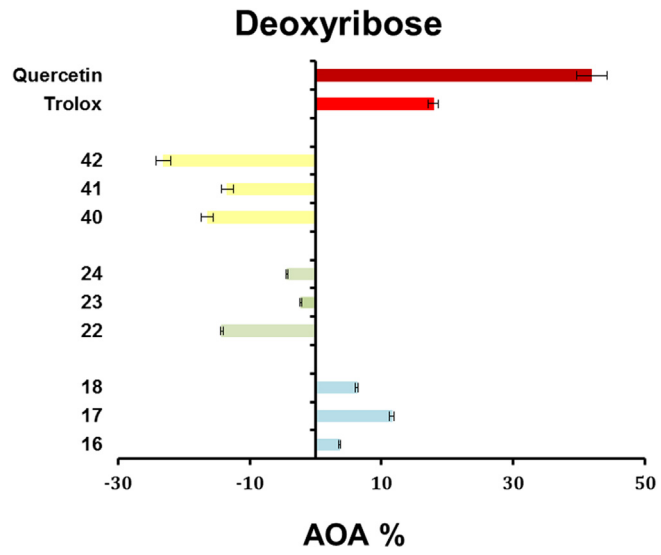


**Fig. 7.** Effect of **16**–**18**, **22**–**24**, **40**–**42** [80 μmol $L^{-1}$] on *in vitro* Fe(II) induced oxidative damage in lipid containing model systems. Trolox and Quercetin at the same concentration have been used as reference compounds.

deoxyribose). All the tested compounds can have protective effect on Fe(II) oxidative stress cellular damage of cellular lipids. The study has revealed **17** as the most potent compound which has demonstrated protection effect in both tested systems. In both systems where protection effect has been observed the obtained results are in the same concentration range as the ones for strong antioxidant reference like Quercetin and Trolox.

### 3.2.4. *Computational study on possible radical scavenging mechanisms and physico-chemical properties of compounds 16-45*

As previously discussed [12], based on structural similarities of 1,3-disubstituted benzimidazole-2-thiones to melatonin, hydrogen atom transfer (HAT) and single electron transfer (SET) are the main mechanisms expected to contribute to their free-radicals scavenging activity:

$$A\text{-}H + ROO^{\bullet} \rightarrow A^{\bullet} + ROOH \text{ (HAT)}$$

$$A\text{-}H + ROO^{\bullet} \rightarrow A\text{-}H^{\bullet+} + ROO^{-} \text{ (SET)}/A\text{-}H^{\bullet+} + ROO^{-} \rightarrow A^{\bullet} + ROOH \text{ (PT)}$$

The efficacy of radical scavenging according to these two mechanisms can can be estimated by calculating the respective reaction enthalpies – bond dissociation entalphy (BDE) and ionization potential (IP) according to the equations [28]:

$$BDE = H(R^{\bullet}) + H(H^{\bullet}) - H(R{-}H)$$

$$IP = H(RH^{+\bullet}) + H(e^{-}) - H(R{-}H)$$

DFT/B3LYP calculations have been successfully used to obtain the reaction enthalpies of a variety of antioxidants [28,37–44] including melatonin derivatives [31], and provided good agreement of calculated values with available experimental data over reasonable computational time. Therefore in our study we have relied on the same computational method.

The computational study has been carried out based on the reaction enthalpies of compound **17** which have shown the highest hepatoprotective and antioxidant activity within the studied hydrazones. The substantially larger number of atoms in **17** has not allowed the use of B3LYP/6–311++G** as in our earlier study on the ester and hydrazide derivatives of 1,3-disubstituted benzimidazol-2-thiones [12], therefore the calculations have been performed by B3LYP/6-31+G* in gas phase and water. For accurate comparison, the BDE and IP values of ester **10** and hydrazide **15**, showing the best protection among the ester and hydrazide derivatives, as well as the model lipid radicals have been calculated at the current level of theory (Table 3).

According to the B3LYP/6-31+G* calculations, for hydrazone **17** there are four possible sites for hydrogen atom abstraction (Fig. 8). Two of them are from the methylene groups between the benzimidazole ring and carbonyl groups at the side N-chains (*site 1, 1′* and *2, 2′*), similarly to the ester and hydrazide derivatives, and also from the amide N–H bond (*site 3,3′*) and methyne C–H (*site 4*). The sites with the lowest BDE and correspondingly the most favorable sites for H abstraction are *1* and *3* with 377 and 365 kJ $mol^{-1}$. The amide N–H bond has shown BDE value higher than the lowest BDE in the ester derivative **10**, but substantially lower than the one in the hydrazide **15** (Table 3). From the calculated BDE values for **17**, it becomes evident that the hydrazones of benzimidazole-2-thiones will be able to scavenge alkoxy radicals (BDE < 400 kJ $mol^{-1}$). This outlines the hydrazones, represented by compound **17**, as worse radical scavengers than the hydrazide derivatives but superior to the ester derivatives according to the HAT mechanism in nonpolar medium.

On the other hand, the water ionization potential of **17** is 316 kJ $mol^{-1}$, considerably lower than the water BDE value for H atom transfer from *site 3*. This indicates the SET mechanism as strongly preferred for manifestation of the antioxidant action of the hydrazone derivatives in water. The data presented in Table 3 demonstrate that the hydrazones possess the highest capacity among the studied benzimidazole-2-thione derivatives to donate single electrons and scavenge the free radicals by SET mechanism. The calculated relaxed IPs of **10**, **15**, and **17** are also in support of this conclusion.

From the computational study on the radical scavenging mechanisms it can be summarized that the hydrazone derivatives will be able to scavenge OH and alkoxy radicals thus exibiting cytoprotective action by inhibition of the lipid peroxidation initiation. Similarly, melatonin is also not considered highly effective as a chain breaking antioxidant [5], but successfully reduces the initiation of LPO.

An effective antioxidant should be able to pass through physiological barriers and be quickly transported to the cells. Therefore the solubility of the studied compounds in lipid and water media has been evaluated by calculation of logP, volume and molecular weight, flexibility, and the presence of hydrogen donors and acceptors using the Molinspiration program [45] (Table 4).

The values of logP of compounds **16**–**45** suggest a higher lipophilicity in comparison to our previously tested esters and

**Table 3**
Bond dissociation entalphies (BDE) at different sites, ionization potentials (IP) and relaxation ionization potential (rIP) calculated by B3LYP/6-31+G* in kJ. $mol^{-1}$.

| Compound | BDE (nonpolar) | BDE (water) | IP (water) | rIP (water) |
|---|---|---|---|---|
| **17** | 377 (*site* 1) | | 316 | 5.69 |
| | 398 (*site* 2) | | | |
| | 365 (*site* 3) | 365 (*site 3*) | | |
| | 409 (*site* 4) | | | |
| **10** | 380 (*site* 1) | 379 (*site 1*) | 327 | 5.80 |
| **15** | 300 (*site 3*) | 318 (*site 3*) | 326 | 5.78 |
| Melatonin | 346 (*indolyl N–H*) | 345 (*indolyl N–H*) | 279 | 5.29 |
| ROH | 406 | | | |
| ROOH | 321 | | | |

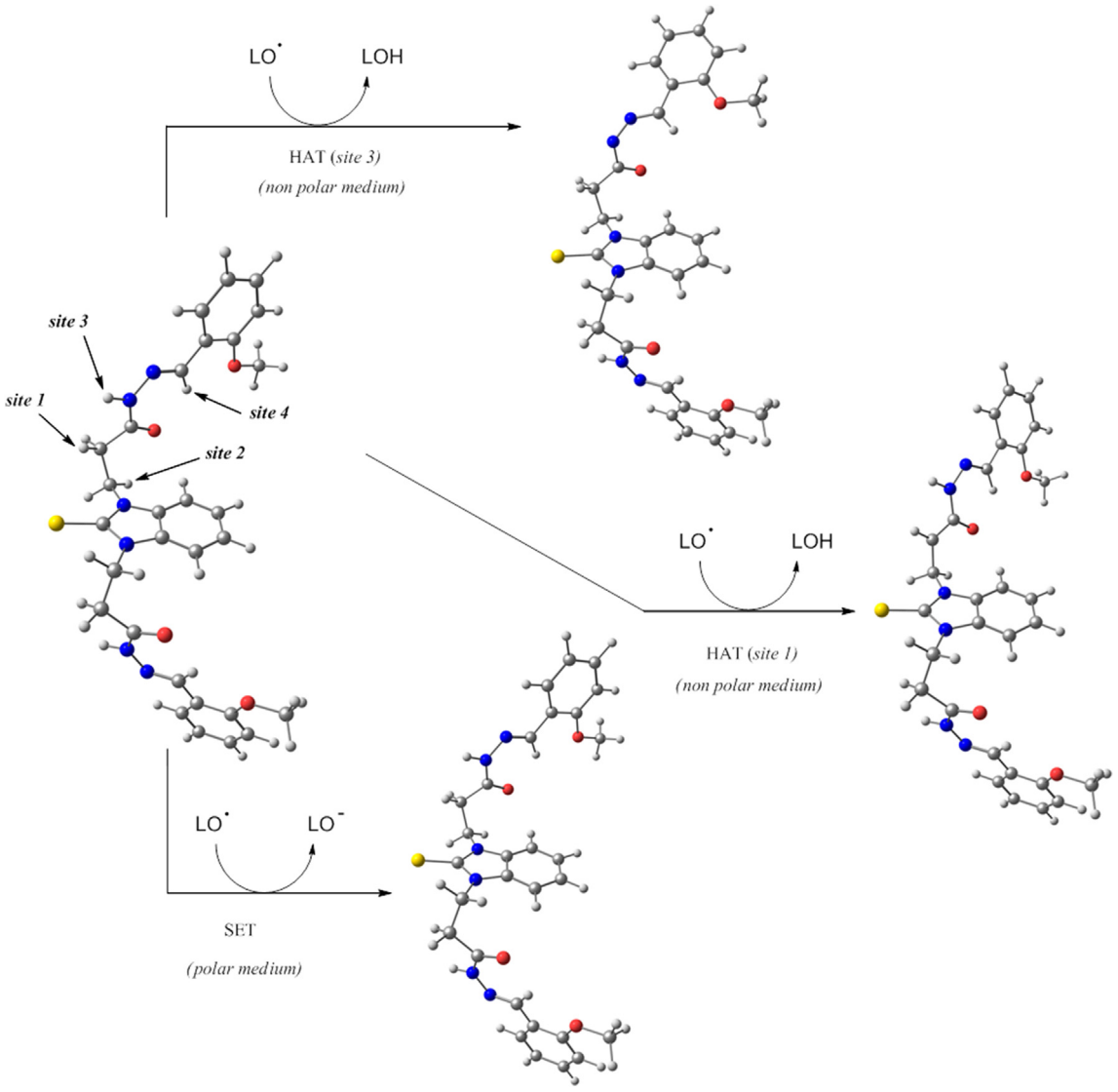


**Fig. 8.** Hydrogen atom abstraction from *site 1* and *3* of **17** and single electron transfer via SET mechanism.

hydrazides which determines their higher affinity to the lipid membrane contributes to their function as cytoprotectors of lipid peroxidation.

## 4. Conclusions

Series of new N,N′-disubstituted benzimidazole-2-thiones with extended side chains have been synthesized by coupling with various benzaldehydes containing methoxy or fluoro groups. By monitoring the effects of the studied compounds on the cell viability and the levels of lactate dehydrogenase, glutathione and malonaldehyde in isolated rat hepatocytes it was shown that the compounds containing unsubstituted benzimidazole-2-thione ring preserve best the functional-metabolic status of the hepatocytes. The evaluation of the antioxidant properties of the compounds using oxidative stress induced by *tert*-butylhydroperoxide (*tert*-BOOH) on rat hepatocytes revealed that the unsubstituted benzimidazole-2-thiones containing methoxyphenyl moieties exhibited statistically significant cytoprotective and antioxidant effects similar to those of quercetin. Comparing the obtained results from the rat hepatocytes containing model systems and the *in vitro*

**Table 4**
Calculated physico-chemical properties of **16**–**45**.

| No | logP[a] | TPSA[b] | $N_{atoms}$[c] | MW[d] | $N_{ON}$[e] | $N_{OHNH}$[f] | $N_{viol.}$[g] | $N_{rotb.}$[h] | Vol[i] |
|---|---|---|---|---|---|---|---|---|---|
| 16, 17, 18 | 3.72 | 111 | 38 | 530 | 10 | 2 | 1 | 10 | 463 |
| **19, 20, 21** | 3.93 | 92 | 36 | 506 | 8 | 2 | 1 | 8 | 422 |
| **22, 23, 24** | 4.14 | 111 | 39 | 545 | 10 | 2 | 1 | 10 | 480 |
| **25, 26, 27** | 4.36 | 93 | 37 | 520 | 8 | 2 | 1 | 8 | 439 |
| **28, 29, 30** | 3.65 | 157 | 41 | 576 | 13 | 2 | 2 | 1 | 487 |
| **31, 32, 33** | 3.87 | 138 | 39 | 551 | 11 | 2 | 2 | 9 | 445 |
| **34, 35, 36** | 4.37 | 111 | 39 | 565 | 10 | 2 | 1 | 10 | 476 |
| **37, 38, 39** | 4.58 | 93 | 37 | 540 | 8 | 2 | 1 | 8 | 436 |
| **40, 41, 42** | 5.24 | 128 | 46 | 634 | 11 | 2 | 3 | 12 | 553 |
| **43, 44, 45** | 5.36 | 109 | 44 | 610 | 9 | 2 | 2 | 10 | 512 |

[a] Octanol-water partition coefficient calculated by the methodology developed by Molinspiration.
[b] Topological surface area.
[c] Number of nonhydrogen atoms.
[d] Molecular weight.
[e] Number of hydrogen-bond acceptors (O and N atoms).
[f] Number of hydrogen-bond donors (OH and NH groups).
[g] Number of "Rule of five" violations.
[h] Number of rotatable bonds.
[i] Molecular volume.

chemical assays of Fe(II) induced oxidative damage we can assume that the observed hepatoprotective effect could be attributed to the capability of the tested compounds to preserve biologically important molecules from oxidative damage.

By protecting the lipids from free radical damage, the studied compounds could help in preserving the morphological and functional integrity of cell membranes, thus helping to maintain the function of the proteins (receptors, channels, pores, etc.) in the cell membranes. Based on calculated physico-chemical properties such as polar surface area, molecular weight, number of rotatable bonds and number of hydrogen-bond acceptors and donors it was found that the studied compounds show favorable properties to function as cytoprotectors of lipid peroxidation.

The mechanisms of the radical scavenging of the tested compounds in nonpolar (lipid) and polar (aqueous) medium were studied based on calculated reaction enthalpies of hydrogen atom abstraction (HAT mechanism) and single-electron transfer (SET mechanism). From the calculated reaction enthalpies it became evident that, similarly to melatonin, the hydrazone derivatives would be able to scavenge hydroxyl and alkoxyl radicals thus exibiting cytoprotective action by inhibition of the lipid peroxidation initiation. In water the SET mechanism is strongly preferred for manifestation of the antioxidant action of the hydrazone derivatives.

The study demonstrated that 1,3-disubstituted benzimidazole-2-thione with extended side chains can be regarded as promising new radical scavengers and oxidative stress inhibitors for the treatment of liver disorders.

## Acknowledgements

The financial support of this work by the National Science Fund of Bulgaria (Contracts RNF01/0110) is gratefully acknowledged.

## Appendix A. Supplementary data

Supplementary data related to this article can be found at https://doi.org/10.1016/j.molstruc.2018.03.119.

## References

[1] S. Li, H. Tan, N. Wang, Z. Zhang, L. Lao, C. Wong, Y. Feng, The role of oxidative stress and antioxidants in liver diseases, Int. J. Mol. Sci. 16 (2015) 26087–26124.
[2] J. Medina, R. Moreno-Otero, Pathophysiological basis for antioxidant therapy in chronic liver disease, Drugs 65 (2005) 2445–2461.
[3] H. Cichoż-Lach, A. Michalak, Oxidative stress as a crucial factor in liver diseases, World J. Gastroenterol. 20 (2014) 8082–8091.
[4] A.M. Mathes, Hepatoprotective actions of melatonin: possible mediation by melatonin receptors, World J. Gastroenterol. 16 (2010) 6087–6097.
[5] R.J. Reiter, D. Tan, A. Galano, Melatonin reduces lipid peroxidation and membrane viscosity, Front. Physiol. 5 (2014) 377–380.
[6] G. Kocic, B. Djordjevic, K. Tomovic, S. Stojanovic, H. Kocic, I. Arsic, D. Sokolovic, A. Smelcerovic, Antioxidative, membrane protective and antiapoptotic effects of melatonin, in silico study of physico-chemical profile and efficiency of nanoliposome delivery compared to betaine, RSC Adv. 7 (2017) 1271–1281.
[7] D.X. Tan, L.C. Manchester, M.P. Terron, L.J. Flores, R.J. Reiter, One molecule, many derivatives: a never ending interaction of melatonin with reactive oxygen and nitrogen species? J. Pineal Res. 42 (2007) 28–42.
[8] P. Guo, H. Pi, S. Xu, L. Zhang, Y. Li, M. Li, et al., Melatonin improves mitochondrial function by promoting MT1/SIRT1/PGC-1 alpha-dependent mitochondrial biogenesis in cadmium-induced hepatotoxicity in vitro, Toxicol. Sci. 142 (2014) 182–195.
[9] R.J. Reiter, D.X. Tan, L.C. Manchester, W. Qi, Biochemical reactivity of melatonin with reactive oxygen and nitrogen species: a review of the evidence, Cell Biochem. Biophys. 34 (2001) 237–256.
[10] R.J. Reiter, L. Fuentes-Broto, S.D. Paredes, D.X. Tan, J.J. Garcia, Melatonin and the pathophysiology of cellular membranes, Marmara Pharm. J. 14 (2010) 1–9.
[11] O. Celik, M. Naziroglu, Melatonin modulates apoptosis and TRPM2 channels in transfected cells activated by oxidative stress, Physiol. Behav. 107 (2012) 458–465.
[12] N. Anastassova, A. Mavrova, D. Yancheva, M. Kondeva-Burdina, V. Tzankova, S. Stoyanov, B.R. ShivachevNikolova, Hepatotoxicity and antioxidant activity of some new N,N′-disubstituted benzimidazole-2-thiones, radical scavenging mechanism and structure-activity relationship, Arab. J. Chem. 11 (2017) 353–369.
[13] H. Gurer-Orhan, H. Orhan, S. Suzen, M.O. Püsküllü, E. Buyukbingol, Synthesis and evaluation of in vitro antioxidant capacities of some benzimidazole derivatives, J. Enzyme Inhib. Med. Chem. 21 (2006) 241–247.
[14] H. Shirinzadeh, B. Eren, H. Gurer-Orhan, S. Suzen, S. Özden, Novel indole-based analogs of melatonin: synthesis and in vitro antioxidant activity studies, Molecules 15 (2010) 2187–2202.
[15] S. Suzen, Melatonin and synthetic analogs as antioxidants, Curr. Drug Deliv. 10 (2013) 71–75.
[16] A.D. Yılmaz, T. Coban, S. Suzen, Synthesis and antioxidant activity evaluations of melatoninbased analogue indole-hydrazide/hydrazone derivatives, J. Enzym. Inhib. Med. Chem. 3 (2012) 428–436.
[17] M.L. Bajt, J.A. Lawson, S.L. Vonderfecht, J.S. Gujral, H. Jaeschke, Protection against Fas receptor-mediated apoptosis in hepatocytes and nonparenchymal cells by a caspase-8 inhibitor in vivo: evidence for a postmitochondrial processing of caspase-8, Toxicol. Sci. 58 (2000) 109–117.
[18] M. Mitcheva, M. Kondeva, V. Vitcheva, P. Nedialkov, G. Kitanov, Effect of benzophenones from Hypericum annulatum on carbon tetrachloride-induced toxicity in freshly isolated rat hepatocytes, Redox Rep. 11 (2006) 3–8.
[19] D. Fau, A. Berson, D. Eugene, B. Fromenty, C. Fisch, D. Pessayre, Mechanism for the hepatotoxicity of the antiandrogen, nilutamide. Evidence suggesting that redox cycling of this nitroaromatic drug leads to oxidative stress in isolated hepatocytes, J. Pharmacol. Exp. Ther 263 (1992) 69–77.
[20] A. Mavrova, K. Anichina, D. Vutchev, Y. Tsenov, M. Kondeva, M. Micheva, Synthesis and antitrichinellosis activity of some 2-substituted-[1,3]thiazolo [3,2-a]benzimidazol-3(2H)-ones, Bioorg. Med. Chem. 13 (2005) 5550–5559.
[21] F. Takayama, T. Egashira, Y. Yamanaka, Protective effect of Ninjin-yoei-to on damage to isolated hepatocytes following transient exposure to tert-butyl hydroperoxide, Jpn. J. Pharmacol. 85 (2001) 227–233.
[22] D. Fau, D. Eugene, A. Berson, P. Letteron, B. Fromenty, C. Fisch, D. Pessayre, Toxicity of the antiandrogen flutamide in isolated rat hepatocytes, J. Pharmacol. Exp. Ther. 269 (1994) 1–9.
[23] I. Sadowska-Bartosz, S. Galiniak, G. Bartosz, Modification of the deoxyribose test to detect strong iron binding, Acta Biochim. Pol. 64 (2017) 195–198.
[24] T. Genaro-Mattos, L. Dalvi, R. Oliveira, J. Ginani, M. Hermes-Lima, Reevaluation of the 2-deoxyribose assay for determination of free radical formation, Biochim. Biophys. Acta 1790 (2009) 1636–1642.
[25] M.J. Frisch, G.W. Trucks, H.B. Schlegel, G.E. Scuseria, M.A. Robb, J.R. Cheeseman, G. Scalmani, V. Barone, B. Mennucci, G.A. Petersson, H. Nakatsuji, M. Caricato, X. Li, H.P. Hratchian, A.F. Izmaylov, J. Bloino, G. Zheng, J. Sonnenberg, M. Hada, M. Ehara, K. Toyota, R. Fukuda, J. Hasegawa, M. Ishida, T. Nakajima, Y. Honda, O. Kitao, H. Nakai, T. Vreven, D.A. Montgomery, J.E. Peralta, F. Ogliaro, M. Bearpark, J.J. Heyd, E. Brothers, K.N. Kudin, V.N. Staroverov, R. Kobayashi, J. Normand, K. Raghavachari, A. Rendell, J.C. Burant, S. Iyengar, J. Tomasi, M. Cossi, N. Rega, J.M. Millam, M. Klene, J. Knox, J.B. Cross, V. Bakken, C. Adamo, J. Jaramillo, R. Gomperts, R. Stratmann, O. Yazyev, A.J. Austin, R. Cammi, C. Pomelli, J.W. Ochterski, R.L. Martin, K. Morokuma, V.G. Zakrzewski, G.A. Voth, P. Salvador, J.J. Dannenberg, S. Dapprich, A. Daniels, O. Farkas, J.B. Foresman, J.V. Ortiz, J. Cioslowski, D.J. Fox, Gaussian 09, Revision A1, Gaussian Inc., Wallingford CT, 2009.
[26] A. Becke, Density functional thermochemistry. III. The role of exact exchange, J. Chem. Phys. 98 (1993) 5648–5652.
[27] C. Lee, W. Yang, G.R. Parr, Development of the Colle-Salvetti correlation-energy formula into a functional of the electron density, Phys. Rev. B 37 (1988) 785–789.
[28] E. Klein, V. Lukes, M. Ilcin, DFT/B3LYP study of tocopherols and chromans antioxidant action energetics, Chem. Phys. 336 (2007) 51–57.
[29] Z. Markovic, D. Amic, D. Milenkovic, J.M. Dimitric-Markovic, S. Markovic, Examination of the chemical behavior of the quercetin radical cation towards some bases, Phys. Chem. Chem. Phys. 15 (2013) 7370–7378.
[30] E. Klein, V. Lukes, DFT/B3LYP study of the substituent effect on the reaction enthalpies of the individual steps of single electron transfer-proton transfer and sequential proton loss electron transfer mechanisms of phenols antioxidant action, J. Phys. Chem. 110 (2006) 12312–12320.
[31] J.R. Johns, J.A. Platts, Theoretical insight into the antioxidant properties of melatonin and derivatives, Org. Biomol. Chem. 12 (2014) 7820–7827.
[32] B.J. Blaauboer, A.R. Boobis, J.V. Castell, S. Coecke, G.M.M. Groothuis, A. Guillouzo, T.J. Hall, G.M. Hawksworth, G. Lorenzon, H.G. Miltenburger, N.V. Rogiers, P. Skett, P. Villa, F.J. Wiebel, The practical applicability of hepatocyte cultures in routine testing, ATLA 22 (1994) 231–241.
[33] Council of Europe, European Convention for the Protection of Vertebrate Animals Used for Experimental and Other Scientific Purposes, CETS No. 123, 1991 [displayed 30 May 2007], available at: http://conventions.coe.int/treaty/Commun/QueVoulezVous.asp?NT=123ECL=ENG.
[34] A. Mavrova, K. Anichina, D. Vutchev, Y. Tsenov, M. Kondeva, M. Micheva, Synthesis and antitrichinellosis activity of some 2-substituted-[1,3]thiazolo [3,2-a]benzimidazol-3(2H)-ones, Bioorg. Med. Chem. 13 (2005) 5550–5559.
[35] D. Kriváková, Z. Cervinková, E. Kmoníčková, H. Lotková, O. Kucera, J. Houstek, Tert-butyl hydroperoxide selectively inhibits mitochondrial respiratory-chain enzymes in isolated rat hepatocytes, Physiol. Res. 54 (2005) 67–72.

[36] N. Hristova-Avakumova, B. Nikolova-Mladenova, K. Yoncheva, V. Hadjimitova, Novel hydrazones - antioxidant potential and stabilization via polysaccharide particles, J. Phys. Conf. 780 (2017), 012004.
[37] J.J. Fifen, M. Nsangou, Z. Dhaouadi, O. Motapon, N. Jaidanec, Solvent effects on the antioxidant activity of 3,4-dihydroxyphenylpyruvic acid : DFT and TD-DFT studies, Comp. Theor. Chem. 966 (2011) 232–243.
[38] M. Najafi, M. Najafi, H. Najafi, DFT/B3LYP study of the substituent effects on the reaction enthalpies of the antioxidant mechanisms of Indole-3-Carbinol derivatives in the gas-phase and water, Comp. Theor. Chem. 999 (2012) 34–42.
[39] J. Lengyel, J. Rimarčík, A. Vagánekc, E. Klein, On the radical scavenging activity of isoflavones: thermodynamics of O–H bond cleavage, Phys. Chem. Chem. Phys. 15 (2013) 10895–10903.
[40] A. Benayahoum, H. Amira-Guebailia, O. Houache, Homolytic and heterolytic O–H bond cleavage in trans-resveratrol and some phenantrene analogs: a theoretical study, Comp. Theor. Chem. 1037 (2014) 1–9.
[41] G. Mazzone, N. Malaj, A. Galano, N. Russoa, M. Toscano, Antioxidant properties of several coumarin–chalcone hybrids from theoretical insights, RSC Adv. 5 (2015) 565–575.
[42] A.V. Zhuravlev, G.A. Zakharov, B.F. Shchegolev, E.V. Savvateeva-Popova, Antioxidant properties of kynurenines: density functional theory calculations, PLoS Comput. Biol. 12 (2016), https://doi.org/10.1371/journal.pcbi.1005213 e1005213.
[43] J. Wang, H. Tang, B. Hou, P. Zhang, Q. Wang, B.-L. Zhang, Y.-W. Huang, Y. Wang, Z.-M. Xiang, C.-T. Zi, X.-J. Wang, J. Sheng, Synthesis, antioxidant activity, and density functional theory study of catechin derivatives, RSC Adv. 7 (2017) 54136–54141.
[44] K. Perez-Cruz, M. Moncada-Basualto, J. Morales-Valenzuela, G. Barriga-Gonzalez, J.A. Squella, P. Navarrete-Encina, C. Olea-Azar, Synthesis and antioxidant study of new polyphenolic hybrid-coumarins, Arab. J. Chem (2017), https://doi.org/10.1016/j.arabjc.2017.05.007.
[45] Molinspiration Cheminformatics, 2016 available at: www.molinspiration.com. Molinspiration property engine v2016.10.